

Numerical Modeling of Atmospheric Temperature and Stratospheric Ozone Sensitivity to Sea Surface Temperature Variability

[Sergei Smyshlyaev](#)*, [Andrew R. Jakovlev](#), Vener Ya. Galin

Posted Date: 2 January 2024

doi: 10.20944/preprints202401.0050.v1

Keywords: sea surface temperature (SST); El-Nino - Southern Oscillation (ENSO); long-term variability; numerical simulation; reanalysis data; stratospheric ozone; stratosphere polar vortex (SPV); residual circulation; wave activity



Preprints.org is a free multidiscipline platform providing preprint service that is dedicated to making early versions of research outputs permanently available and citable. Preprints posted at Preprints.org appear in Web of Science, Crossref, Google Scholar, Scilit, Europe PMC.

Copyright: This is an open access article distributed under the Creative Commons Attribution License which permits unrestricted use, distribution, and reproduction in any medium, provided the original work is properly cited.

Article

Numerical Modeling of Atmospheric Temperature and Stratospheric Ozone Sensitivity to Sea Surface Temperature Variability

Sergei P. Smyshlyaev^{1,2}, Andrew R. Jakovlev^{1,2,*} and Vener Ya. Galin³

¹ Department of meteorological forecasting, Russian State Hydrometeorological University, 79 Voronezhskaya str., 192007 St. Petersburg, Russia; smyshl@rshu.ru

² Physics Faculty, Saint-Petersburg State University, 3 Ul'yanovskaya str., 3, 198504 St. Petersburg, Russia

³ Institute of Numerical Mathematics RAS, Gubkina Str., 8, 119991 Moscow, Russia; venergalin@yandex.ru

* Correspondence: smyshl@rshu.ru; Tel.: +7-(911)-2765808

Abstract: The results of numerical experiments with the chemistry-climate model of the Institute of Numerical Mathematics of the Russian Academy of Sciences - Russian State Hydro-Meteorological University (INM-RSHU CCM) in comparison with the MERRA2 reanalysis data are presented. To assess the impact of sea surface temperature (SST) on stratospheric processes and the ozone layer, numerical experiments were carried out for scenarios corresponding to the El Niño and La Niña Southern Oscillation phases. It is shown that the El Niño phase contributes to the enhancement of heat and mass transfer to the polar stratosphere, which strengthens the Brewer-Dobson circulation and the flux of wave activity that affect the zonal wind. As a result, during El Niño, the probability of sudden stratospheric warming increases and the stratospheric polar vortex (SPV) weakens, resulting in an increase in total polar stratospheric ozone. The La Niña phase, on the contrary, is accompanied by a weakening of heat and mass transfer from the troposphere to the stratosphere, as a result of which the stratospheric polar vortex strengthens and the total column ozone decreases. It is shown that the effect associated with the Southern Oscillation is more pronounced in the Northern Hemisphere than in the Southern Hemisphere. Numerical experiments were also carried out for scenarios in which the sea surface temperature was set corresponding to the early 1980s, and the results were compared with calculations in which the SST was set corresponding to the late 2010s. This allowed us to assess the influence of the multiyear trend in the SST increase on stratospheric processes and the ozone layer. It was shown that the SST increase is most pronounced in the Arctic, which corresponds to the phenomenon of "Arctic amplification", and therefore, the heat and mass transfer to the stratosphere increases in the Northern Hemisphere, which contributes to some weakening of the SPV and increase of the total column ozone. But, compared to the Southern Oscillation, the influence of the SST trend on the SPV and total column ozone is much weaker and is observed mainly in the Northern Hemisphere.

Keywords: sea surface temperature (SST); El-Nino - Southern Oscillation (ENSO); long-term variability; numerical simulation; reanalysis data; stratospheric ozone; stratosphere polar vortex (SPV); residual circulation; wave activity

1. Introduction

Climate changes are accompanied by changes in sea surface temperature (SST), which, in turn, affect climate changes. At the same time, the climate changes (trend) of SST are superimposed on its interannual fluctuations associated primarily with the El Niño-Southern Oscillation (ENSO) phenomenon. These and other changes in SST lead to changes in the exchange of heat and mass between the atmosphere and the ocean, which affects the surface air heating, vertical heat and mass fluxes, the general atmospheric circulation and, consequently, the weather, climate and chemical composition of the atmosphere not only in the lower but also in the middle atmosphere [1,2]. The study of the peculiarities of the influence of SST variability on the temperature and gas composition of the lower and middle atmosphere in different latitude zones opens great opportunities for a better

understanding of the nuances of climate change against the background of short-term changes in the state of the atmosphere and ocean. At present, all these problems are highly topical [1–4].

The most prominent manifestation of interannual changes in SST is the El Niño-Southern Oscillation (ENSO), when, in the tropical Pacific Ocean, SST increases by several degrees relative to the neutral phase (El Niño) or decreases (La Niña), creating the potential for rapid changes in ocean-atmosphere heat and mass exchange, changes in vertical fluxes, general atmospheric circulation, and wave activity. Long-term changes in SST in recent decades are associated with overall global warming, part of which is an increase in SST by a few tenths of a degree from the early 1980s to the late 2010s across the globe [12], which also creates potential changes in general atmospheric circulation, temperature, and ozone content in different regions of the Earth.

SST changes have a significant impact on the tropospheric temperature both directly in the area of SST variability and indirectly in remote regions of the globe due to the influence on the heat and mass transport and the general atmospheric circulation. In addition, SST changes also affect the stratospheric structure and composition by influencing the vertical heat and mass fluxes, which, in turn, affect the general circulation of the stratosphere. The influence of SST variability on the stratosphere of polar regions is of particular interest, since the change in the general atmospheric circulation affects the stability of the stratospheric polar vortex (SPV). In a stable polar vortex, the exchange of heat and mass between polar and middle latitudes is limited, as a result of which the temperature inside the polar vortex at stratospheric heights decreases and the ozone content decreases [5–7].

The stability of the SPV is characterized by the zonal wind speed in the lower stratosphere at the boundary of polar and mid latitudes. At large values of zonal wind, most of the warm and ozone-rich air from the middle latitudes is carried away by the zonal flow around the polar zone and does not penetrate inside the polar region. Changes in the SST in the tropics and other regions affect the general atmospheric circulation, which can lead to both an increase in zonal wind speed at the SPV boundary, i.e., an increase in SPV stability, and a decrease in zonal wind speed at the polar boundary, i.e., a weakening of SPV stability. The main factors related to the SST variations affecting the zonal flow at the SPV boundary may be the change in the residual circulation determining the Brewer-Dobson circulation in the stratosphere and, consequently, the heat and mass flux across the SPV boundary, as well as the change in wave activity slowing down the zonal flow in the polar boundary region [8–11].

Studies of the atmosphere-ocean interaction have a long history [5–7,13,14], with special attention paid to the influence of ENSO on changes in the temperature and gas composition of the atmosphere. In particular, it was shown that sea warming during the El Niño phase leads to weakening of the Walker circulation and trade winds, which creates the possibility of feedback and influence of these changes on ENSO [12]. In [13], the importance of meridional transport in the tropical zone and zonal transport at the boundary of the Southern Oscillation zone with the influence of Kelvin and Rossby waves was shown.

The problem of ocean influence on the dynamics and gas composition of the stratosphere, including the polar regions, has also been the subject of scientific research over the last decades [8–11,15–18]. It has been shown [9–11] that changes in the SST have a significant effect on the temperature and gas composition of the stratosphere in the polar regions. It has also been shown [8] that zonal wind speed determines the stability of the SPV, with lower mean values of zonal wind in the Arctic than in the Antarctic and, on the contrary, greater interannual variations. A study of the variability of planetary waves showed that the stability of the SPV is determined by the stability of the zonal transport of air masses, whereas an increase in the meridional transport leads to the instability of the SPV [16]. It was also shown that planetary waves are one of the key factors affecting the existence of SPV in the Northern Hemisphere. The influence of meridional SST gradients on the atmospheric circulation and ozone content is shown in [17].

A study of the connection between ENSO and atmospheric circulation has shown that ENSO affects the global circulation both in the troposphere [18,19] and in the stratosphere [20,21]. The El Niño phase leads to an acceleration of the vertical and meridional transport of ozone from the tropical

stratosphere to the middle and polar latitudes, called the Brewer-Dobson circulation, and a warming of the polar stratosphere [22,23]. The Brewer-Dobson circulation is the main transport process for stratospheric ozone [24,25]. The coincidence of the peak period of the Brewer-Dobson circulation with convection due to ENSO in the troposphere during the winter months allows us to link zonal air transport (Walker circulation) with meridional transport in the lower stratosphere [26]. El Niño events lead to a deepening of the Aleutian Minimum [27], which, in combination with standing waves, results in increased wave flux into the stratosphere [28,29]. These vertical waves contribute to sudden stratospheric warming (SSW) events [30,31]. La Niña events contribute to weaker heat and mass flux into the stratosphere, resulting in stronger zonal flow and SPVs, and lower stratospheric air temperatures in the Arctic [32], but the frequency of SSW is not reduced [21,33]. This is due to the fact that during La Niña, a North Pacific ridge appears that does not reach the subarctic Pacific Ocean where it could interact with standing waves [34], and this ridge blocks the flows associated with La Niña, which could further enhance the SPV [34].

During El Niño years, wave activity can increase in winter and, as a consequence, waves propagate into the stratosphere, causing weakening of the SPV in late winter and destruction of the SPV in spring [35–37]. While the impact on the North American winter climate is directly related to these waves, SPV destruction occurs in Europe and Asia [38,39]. The main response of the stratosphere to an increase in SST during the El Niño phase is to weaken the SPV [40]. Typically, from November to mid-January, the SPV is stable during any phase of ENSO, but in late winter, upward propagating planetary waves can lead to a weakening of the SPV [40]. During the El Niño phase, the amplitudes of planetary waves are most often higher than during the La Niña phase, and as a result, they can more intensively destroy the SPV near the end of winter [40].

Climate models are improving their ability to reproduce the phases of the Southern Oscillation and its influence on polar processes [41–43]. In particular, calculations carried out using an improved INM model showed that winter seasons with the El Niño phase are characterized by higher temperatures in the Arctic stratosphere compared to the La Niña phase [43]. These studies also showed that an increase in SST in the North Pacific Ocean (Pacific Subarctic Oscillation) leads to a decrease in temperature in the Arctic stratosphere, and this oscillation is not associated with ENSO. The temperature of the lower stratosphere in the Arctic during the El Niño phase is higher, and the SPV is weaker than during the La Niña phase [21]. During the El Niño phase, the temperature in the Arctic stratosphere is 2 K higher, and the zonal wind speed is 5 m/s lower than during the La Niña phase. According to the study, this may be due to an underestimation of the frequency of SSWs in January. It is known that in the winter months, planetary waves with zonal wave numbers 1 and 2 predominate with maximum amplitudes at 60–70°N latitude. It has been shown that during the El Niño phase in the Arctic stratosphere, the amplitude of wave number 1 increases, and during La Niña, the amplitude of wave number 2 increases [43]. However, the models do not reproduce SSWs associated with La Niña phenomena; they are detected from reanalysis data [33,34].

In addition to ENSO, a significant influence on the atmosphere is exerted by the multiyear positive trend of SST. This trend is largely determined by global warming, which is associated with an increase in greenhouse gases, resulting in warming in the lower troposphere and cooling in the stratosphere [2,42–47]. As studies with the NCAR CCSM3.5 climate model show, changes in greenhouse gases can also affect ENSO [60]. The influence of the multiyear trend of SST, according to the "Arctic amplification" hypothesis, is significant in the Northern Hemisphere [48,49]. Also, the Arctic amplification contributes to the increase of ozone in the Arctic stratosphere [46,47]. Thus, the multiyear trend can also have an impact on the zonal wind, the Brewer-Dobson circulation, and the wave activity flux.

Previous studies have shown that an increase in SST during the El Niño phase, as well as due to the SST trend, contribute to an increase in stratospheric heat fluxes and a weakening of the SPV, while the La Niña phase, corresponding to a decrease in SST in the tropics, contributes to a strengthening of the SPV. The weakening of the SPV can be associated with an increase in the wave activity flux [48,49], whereas the strengthening of the SPV is associated with a weakening of the wave activity flux. That is, the El Niño phase and the increase in SST due to the trend may enhance the flux of wave

activity, while La Niña may weaken it. Despite the fact that the main mechanisms of the influence of SST variability on stratospheric processes are already clear, there are still many questions related to the influence of SST changes on the atmospheric circulation, especially with quantitative estimates, mechanisms of changes in the meridional and zonal components of the atmospheric circulation, and their influence on the stability of SPV, stratospheric temperature and ozone content.

In this study, as a follow-up to previous studies, both multiyear SST changes and interannual SST changes determining the interannual variability of atmospheric temperature and ozone content are considered. Based on the analysis of the results of numerical experiments performed with the chemical-climatic model for different SST scenarios corresponding to different conditions of SST changes due to ENSO and long-term trends, the sensitivity of tropospheric and stratospheric temperature and ozone content as a function of SST changes is evaluated. Chapter 2 describes the methodology, model, input data, and reanalysis data. Chapter 3 describes the analysis of SST changes, numerical experimental results and reanalysis data for El Niño and La Niña scenarios and for the beginning and end of the period from 1980 to 2020. Chapter 4 provides a discussion. Chapter 5 summarizes the conclusions.

2. Materials and Methods

To analyze the sensitivity of atmospheric temperature and ozone to SST variability, the technique of numerical experiments with a chemistry-climate model (CCM) was used, the results of which were compared with reanalysis data.

For numerical experiments, we used the CCM developed at the Institute of Numerical Mathematics of the Russian Academy of Sciences and the Russian State Hydrometeorological University (INM RAS – RSHU CCM) [16,50–52]. The model consists of two parts: a dynamic part, which calculates meteorological variables; and a chemical part, which calculates atmospheric gas parameters. The dynamic part of the model includes the basic equations of hydrodynamics and thermodynamics of the atmosphere, which are solved by finite difference methods and used to calculate the values of the main meteorological parameters. The resolution of the INM RAS – RSHU CCM is 4x5 latitude/longitude. The model grid is from 175°W to 180°E and from 88°S to 88°N. Vertically, the number of model σ levels is 39 (from the surface to the 0.003 hPa level, which approximately corresponds to the altitudinal interval from the surface to the mesopause). The number of grid points in the model is 72 in longitude and 45 in latitude. The exchange between the dynamic and chemical blocks is carried out every 6 hours (4 times a day).

The evolution of trace gases is described using their transport equations, which are also solved by finite difference methods, and determine the rates of chemical reactions. In addition to basic meteorological parameters, the CCM calculates the variability of 74 species of gases in the lower and middle atmosphere for 174 chemical reactions in the gas phase and heterogeneous reactions, as well as 46 photolysis processes, including oxygen, nitrogen, hydrogen, chlorine, bromine, and hydrocarbon cycles [53–55]. The model includes processes of polar stratospheric cloud formation and evolution based on the distribution of sulfur aerosol in the stratosphere [54,55]. The dynamics of the polar vortex is calculated in the dynamical part of the CCM [55]. First, solar radiation fluxes are calculated taking into account ozone content and molecular light scattering [54]. These fluxes are used to calculate the rates of photodissociation of gases, from which the rates of photochemical gas formation are calculated. In this case, the temperature values calculated in the dynamic part of the model are used for the calculation. Such rates of chemical reactions make it possible to simulate the evolution of ozone and other gases [53].

The influence of SST and sea ice coverage (SIC) is taken into account in the dynamical part of the CCM as the lower boundary condition of the thermodynamic equation. The mean monthly SST and SIC data used from the Met Office reanalysis data [56] were interpolated to mean daily values and used to set the temperature at the lower boundary of the model at those points of the model grid that fall on the ocean.

At the first stage of numerical experiments, the calculation with the CCM was performed for the climatic period from 1980 to 2020, in which the interannual variability of the factors influencing the

temperature change and chemical composition was set: greenhouse gas content, sea surface temperature and its ice coverage area, atmospheric aerosol content, and variability of solar activity fluxes. The results of calculations were compared with the MERRA2 reanalysis data. Particular attention was paid to the variability of temperature and ozone content in relation to the variability of ocean surface temperature in the tropical Pacific Ocean, both as a result of the long-period trend (trend) and interannual variations associated with ENSO phases. The purpose of these experiments was to determine the influence of SST variability against the background of the role of other factors and, first of all, the greenhouse gas content on the state of the lower and middle atmosphere.

In the second stage of the numerical experiments, calculations with CCM were performed for several scenarios, in which we set repeated annual cycles of SST changes corresponding to each year from 1980 to 2020. Each scenario was calculated for 30 years. The results of calculations for the last 5 years were averaged and, depending on the classification, were assigned to one of four classes: the beginning of the climatic period with a neutral ENSO phase, the end of the climatic period with a neutral ENSO phase, the El Niño phase, and the La Niña phase. The purpose of this stage of numerical experiments was to isolate the influence of SST on temperature and ozone content with other influencing factors unchanged. The calculations were performed from the beginning of 2020 with a repeating seasonal cycle for 2020 for all parameters except SST and SIC. Thus, the results of calculations showed the response of the lower and middle atmosphere temperature and ozone content only to the changes of SST and SIC.

The results of calculations for scenarios corresponding to the most powerful positive and negative SST deviations in the tropical Pacific Ocean were especially highlighted. These were 1983, 1998, and 2016, corresponding to the most powerful phase of El Niño, and 1989, 2000 and 2011, corresponding to the most powerful phase of La Niña [12,57,58]. For the analysis, differences in mean values for El Niño years and La Niña years for SST and atmospheric characteristics were calculated. Thus, the average calculated values of atmospheric parameters corresponding to the El Niño phase were compared with the average values corresponding to the La Niña phase. In addition, a similar comparison was carried out for years corresponding to the beginning of the climatic period and the neutral phase of ENSO (1981, 1982 and 1986), as well as the end of the climatic period and the neutral phase of ENSO (2014, 2017 and 2020) [12]. Comparison of the results of calculations of average values for these years at the beginning and end of the climatic period was used to analyze the influence of the SST trend on atmospheric parameters. The results of model calculations were compared with data from the Modern Age Retrospective Analysis for Research and Applications Version 2 (MERRA2 [59]) reanalysis for the period 1980-2020.

3. Results

3.1. Annual and long-term changes in SST

Figure 1 (left) shows the difference in SST between the three years with the most pronounced El Niño and La Niña phases according to Met Office data. As expected, the maximum difference between the ENSO phases is observed in the tropical and subtropical parts of the Pacific Ocean. Moreover, while in the tropics there is a significant excess of up to 4 degrees for the El Niño phase compared to the La Niña phase, in the subtropics, on the contrary, the SST during the El Niño phase is up to 2 degrees lower than during the La Niña phase. Such temperature differences have the potential to influence both sea currents and SST changes in other regions, as well as atmospheric circulation through changes in vertical temperature gradients.

Figure 1 (right) shows the Met Office SST differences between the end and beginning of the 1980-2020 climate period. As can be seen, at the end of the period the global average SST is 0.5-1.0 degrees Celsius higher than at the beginning of the period, which is most likely due to an increase in greenhouse gases. The exception is the area of the Pacific Ocean near South America, where a 1.0 degree decrease in SST is observed, indicating ocean cooling in the ENSO zone over the last 40 years. Also a decrease of SST by the end of the period is observed near the Antarctic. This decrease in SST may be related to the melting of Antarctic ice, which brings cold fresh water into the ocean. Also the

decreased SST in some areas (especially in the tropics near Africa and Indonesia) can be connected with the increased cyclonic activity and increased cloudiness and precipitation in these areas. In addition, areas of strong increase in SST in the polar zones attract attention both when comparing ENSO phases and when comparing the end and beginning of the climatic period. These areas of strong SST difference can be related to the difference in the area of sea ice coverage, since only the SST in cells with free water in at least half of the cell area was taken into account.

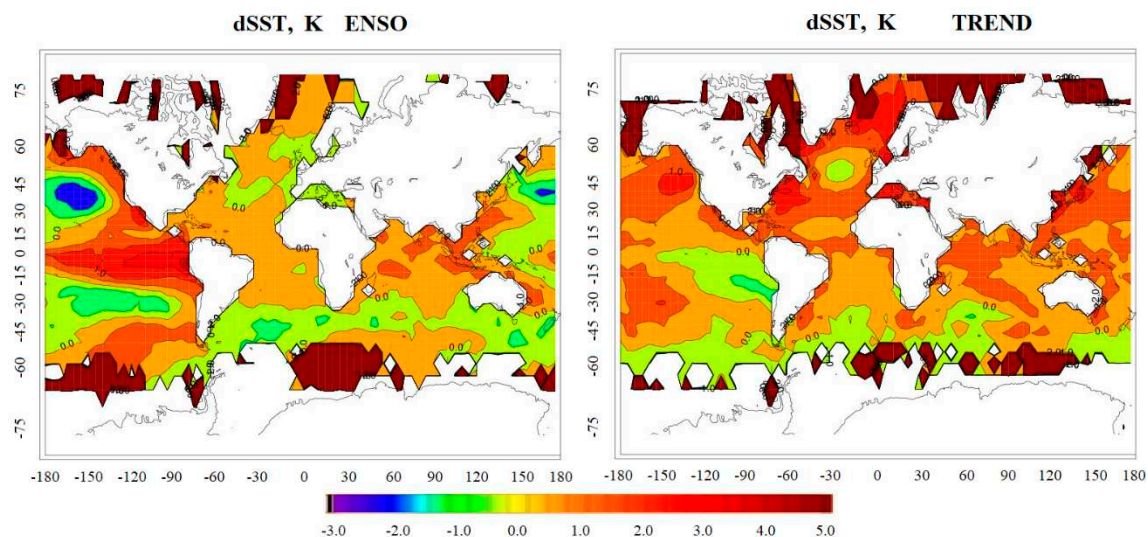


Figure 1. Mean SST difference (degrees) between 3 years of El Niño (1983, 1998 and 2016) and 3 years of La Niña (1989, 2000 and 2011) (left) and between 3 years with neutral ENSO phase at the end of the climate period (2014, 2017 and 2020) and 3 years at the beginning of the period (1981, 1982 and 1986) from Met Office reanalysis data (right).

Comparison of the SST differences for different ENSO phases, as well as for the end and beginning of the considered climatic period, shows that due to changes in both the horizontal and vertical air temperature gradients due to the influence of the underlying sea surface, the heat and mass fluxes between the ocean and the atmosphere may change to different degrees in different regions of the Earth. This can affect heat and mass transport both between neighboring regions and in the vertical direction. In addition, changes in the regional circulation also affect the general atmospheric circulation, creating the potential for remote effects. In the present work, special attention is paid to the influence of SST variability, which, as can be seen from Fig. 1, is maximal in tropical and subtropical regions, if we ignore artifactual changes in polar regions due to different ice coverage, on processes in polar regions.

Figure 2 presents the altitudinal variability of atmospheric temperature anomalies compared to the average values for the period 1980-2020. Fig. 2a and 2c present the MERRA-2 reanalysis data for the tropics and global scale, respectively, and Fig. 2b and 2d present similar results obtained from calculations using the INM RAS-RSHU CCM. The modeling results, in general, agree quite well with the reanalysis data both in the tropical zone and on a global scale. Both reanalysis and CCM data show warming during the study period up to tropopause heights (temperature increase by 0.5-1.0 degrees Celsius from 1980 to 2020 at heights up to 15-17 km), and stratospheric cooling (temperature decrease by 1.0-1.5 degrees Celsius above the tropopause). Against the background of the general trend, one can also observe temperature anomalies in the 0-20 km layer associated with ENSO, which are more pronounced in the tropical zone (Figures 1 and 2), but they are also visible on a global scale (Figures 3 and 4). It can be seen that both the positive anomalies of atmospheric temperature associated with the El Niño phase and its negative anomalies associated with the La Niña phase are more strongly manifested not near the surface, where heat exchange with the sea takes place, but at heights of about 10 km. This effect is noticeable not only in the tropics, where it can be explained by the developed convective motions, but also in the extratropical latitudes, which once again

emphasizes the role of the circulation processes affecting long-range communications in the atmosphere.

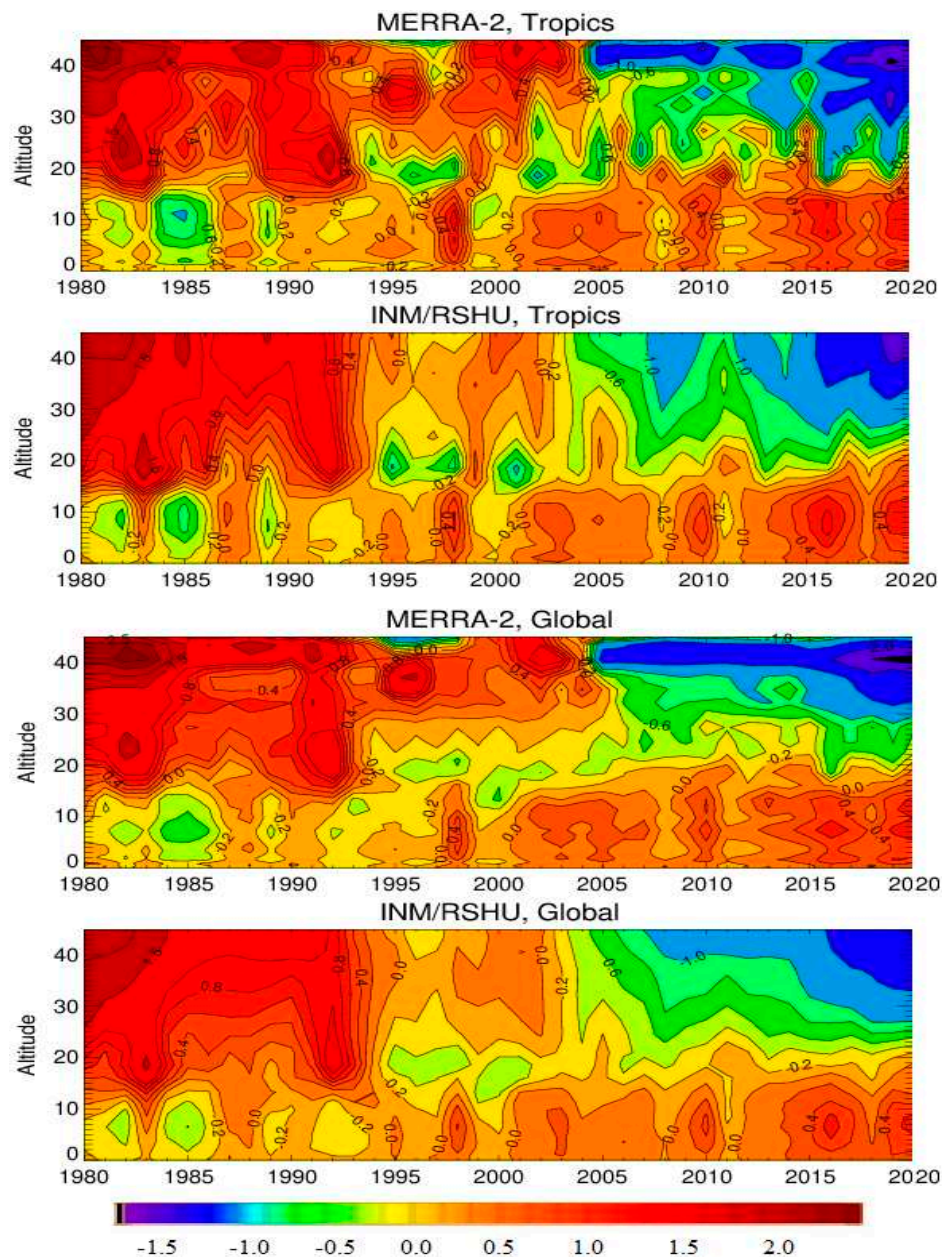


Figure 2. Atmospheric temperature anomalies (in degrees) in the troposphere and stratosphere of the tropical zone from the MERRA-2 reanalysis (1 diagram) and numerical experiments with CCM INM RAS - RSHU (2 diagram), and on a global scale from the MERRA-2 reanalysis (3 diagram) and numerical experiments with CCM INM RAS - RSHU (4 diagram).

The noted different changes in the SST in different latitude and longitude belts can influence the changes in the general atmospheric circulation, heat and mass transport, and, consequently, the temperature and gas composition of the atmosphere, which confirms the previous studies [12,57,58], also the air temperature data are in full agreement with the reanalysis data, which is also shown in [12,57,58]. To analyze the sensitivity of atmospheric parameters to short- and long-term changes in the SST, the following sections present the CCM-calculated changes in temperature, ozone content, and dynamical parameters affecting heat and mass transport and the polar vortex.

Figure 3 (left) presents air temperature differences in the lower troposphere based on modeling results for scenarios with El Niño and La Niña phases. As can be seen, there is a 2-3 degree increase

in air temperature in the equatorial Pacific Ocean, and a 0.6-1 degree decrease at 20-45 latitudes in the Pacific Ocean during El Niño. There is also a powerful 3 degree increase over Alaska, and a 1 degree excess over the Pacific Ocean near Antarctica. This means that during El Niño there is a strong atmospheric heat flux in the equatorial Pacific and over the Arctic, and a weaker one over Antarctica. This may indicate a deepening of the Aleutian Minimum in the Northern Hemisphere due to El Niño, as well as an enhanced heat flux to the Arctic stratosphere. The warming of the troposphere during El Niño leads to the intensification of temperature contrasts between the tropics and polar latitudes, which contributes to the intensification of cyclonic activity in the middle latitudes of the Pacific Ocean. The heat trapped in the upper troposphere by cyclones can penetrate into the lower stratosphere and contribute to HSP. It can also be seen that the air temperature decreases by 0.6 degrees in the Atlantic near Greenland, and by 0.5 degrees in the Atlantic near Antarctica, and by 1.0 between Australia and Antarctica.

Figure 3 (right) shows the differences of air temperature in the troposphere based on the modeling results for the end and beginning of the trend scenarios. As can be seen, an increase in air temperature of 0.6-1 degrees Celsius is observed over most of the planet. However, in the area of Antarctica and to the west of South America there are centers of air temperature decrease by 0.6-1 degrees Celsius, as well as near Antarctica in the area of Australia (by 2 degrees Celsius). This means that, on average on the planet, there is warming in the troposphere. The strongest increase in air temperature (by 1.5-2 degrees) is observed in the Arctic, which indicates the so-called "Arctic amplification" [46,47]. In general, tropospheric air temperature correlates well with SST, (Figure 2, top) the correlation coefficient is 0.9. This indicates that changes in SST play a key role in changes in tropospheric air temperature - as SST increases, the troposphere warms. This is due to the fact that an increase in SST contributes to increased heat fluxes into the atmosphere and convection, resulting in climate warming.

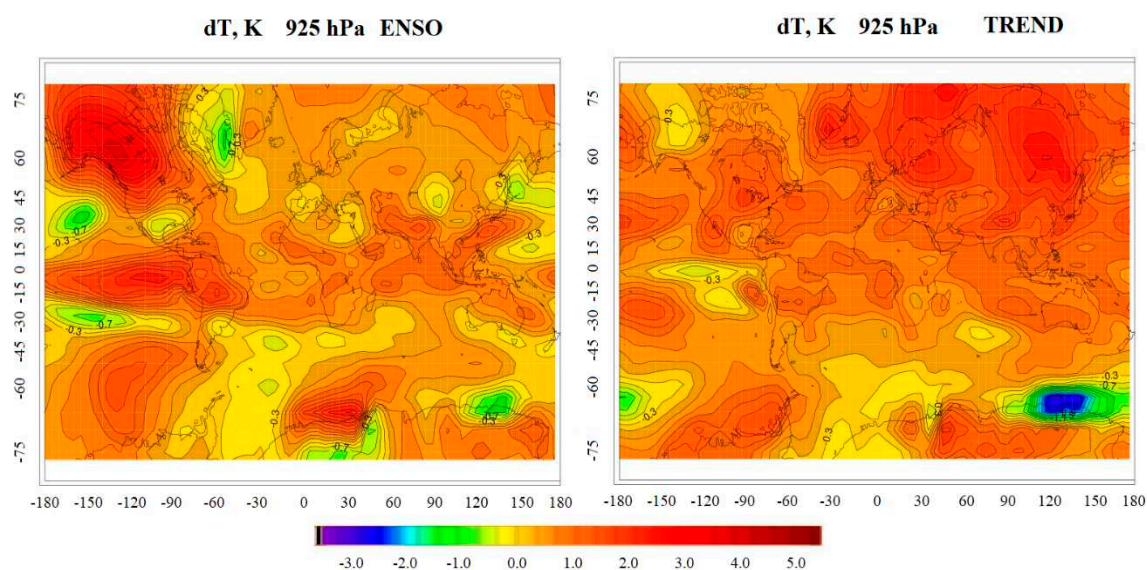


Figure 3. Lower tropospheric temperature between 3 years of El Niño (1983, 1998 and 2016) and 3 years of La Niña (1989, 2000 and 2011) (left) and between 3 years with ENSO neutral phase at the end of the climate period (2014, 2017 and 2020) and 3 years at the beginning of the period (1981, 1982 and 1986) from CCM simulations (right).

3.2. Impact of ENSO on stratospheric processes

This chapter presents the results of numerical experiments using the INM RAS-RSHU CCM. In these experiments, the SST data for the years El Niño and La Niña were used, and the differences of the mean values for El Niño and La Niña were calculated. The other factors (solar activity, changes in the gas composition of the atmosphere due to emissions and absorptions, etc.) were fixed at the

2020 level. This makes it possible to conduct a pure experiment allowing us to evaluate the influence of ENSO on the stratospheric processes.

Figure 4 (row 1) presents vertical profiles of air temperature differences based on modeling results for scenarios with the El Niño phase and the La Niña phase. As can be seen, all year over the tropical region there is an increase in temperature by 5 degrees at altitudes up to 15 km, then at altitudes from 10 to 20 km - a decrease by 0.5 degrees. These regions change little throughout the year, which is due to the constant heat flux from the ocean to the atmosphere in the tropical region during the El Niño phase of the year, whereas this flux is strongly attenuated during La Niña years. In the Arctic stratosphere (60-90 latitudes) during the winter months there is an increase of 1-2 degrees at altitudes of 10-40 km, and a decrease in temperature of 1 degree at altitudes of 50-60 km. This is due to the fact that during the El Niño phase, the heat flux into the stratosphere increases, resulting in an increase in meridional transport from the equator to the North Pole and a deepening of the Aleutian Minimum due to an increase in the temperature contrast between the tropics and the Arctic, which affects the zonal wind and contributes to an increase in the heat flux into the Arctic stratosphere and the SSW [41]. As a result of these processes, air temperature decreases in the tropical stratosphere while it increases in the Arctic stratosphere. These heat fluxes weaken zonal transport and contribute to the instability of the SPV.

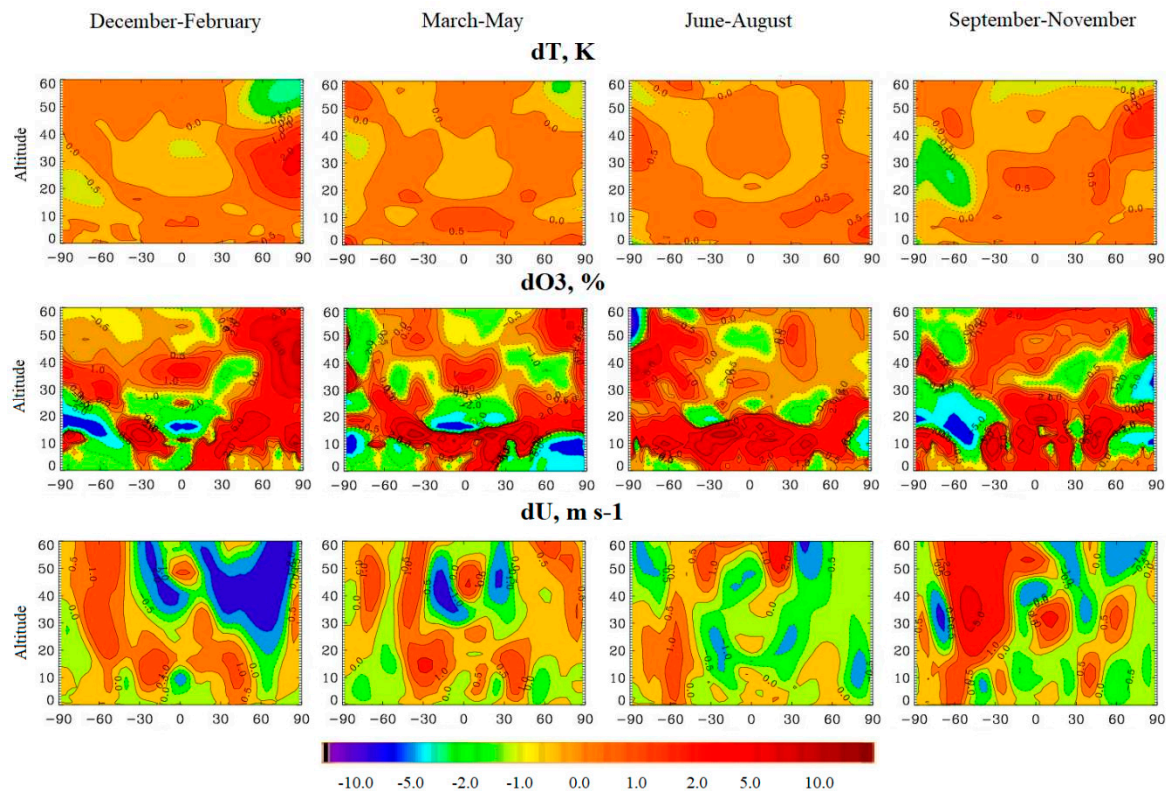


Figure 4. Vertical zonal average profiles of differences in air temperature (1st row), ozone concentration (2nd row) and zonal wind speed in m/s (3rd row) based on modeling results for scenarios with El Niño and La Niña phases.

During spring, the area of temperature increase over the Arctic reduces. At altitudes of 10-20 km at this time, the air temperature decreases by 0.2 degrees. Also during the spring months there appears a similar temperature decrease in the Southern Hemisphere by 0.2 degrees at the altitudes of 20-40 km. In the summer months, one can observe the temperature increase by 0.5 degrees above the Antarctic at the altitudes of 25-45 km and decrease by 0.2 degrees at the altitudes of 50-60 km, with the area of temperature increase being smaller in area than in the Northern Hemisphere, indicating a weaker stratospheric heating in the Southern Hemisphere compared to the Northern Hemisphere.

during the El Niño phase. In the Southern Hemisphere, zonal transport and SPV are much stronger than in the Northern Hemisphere, which is related to the geography of Antarctica, and therefore the stratospheric heat fluxes associated with El Niño are less likely to reach the Antarctic stratosphere and contribute to weaker SPV and a slight weakening of zonal transport. In the autumn months, there are temperature changes similar to the spring ones, only from the Southern Hemisphere to the Northern Hemisphere, with a temperature excess of 1 degree above the Arctic at the altitudes of 30-50 km. This means that during the El Niño phase, the most powerful heat inflow goes to the Arctic stratosphere, which contributes to stratospheric heating, HSP and instability of the SPV, while in the Southern Hemisphere the SPV is usually very stable, and stratospheric heating there is much weaker than in the Northern Hemisphere.

Figure 4 (row 2) presents vertical profiles of ozone concentration differences based on modeling results for the El Niño and La Niña scenarios. As can be seen, ozone concentration agrees with air temperature - over the tropical region there is a decrease in ozone concentration by more than 2% at altitudes of 10-30 km throughout the year. Also a decrease by 1% is observed at 30-60 latitudes at altitudes of 30-50 km. In the Arctic stratosphere during the El Niño phase, ozone concentration is 5% higher than during the La Niña phase, with the difference decreasing to 1-2% in spring, while at 30 km altitude there is a 1% decrease in concentration. This indicates that the heat flux into the stratosphere due to El Niño contributes to enhanced meridional transport, which weakens the zonal wind and contributes to weakening the SPV. As a result, the Brewer-Dobson circulation is enhanced, which contributes to the transport of air temperature and ozone from the tropics to the Arctic stratosphere. As a result, the ozone concentration decreases in the tropical region, while it increases over the Arctic. In the Southern Hemisphere, ozone concentration increases by 2% in the spring months and 5% in the summer months, with the area of increase in ozone concentration in the Southern Hemisphere being smaller than in the Northern Hemisphere. This means that ozone holes are more pronounced in the Southern Hemisphere and during the La Niña phase than in the Northern Hemisphere. At the same time, they exist longer in the Southern Hemisphere. It can also be seen that during the El Niño phase there is an increase in ozone transport from the tropical stratosphere to the Arctic and Antarctic through the Brewer-Dobson circulation, and the ozone transport in the Northern Hemisphere is stronger than in the Southern Hemisphere, where the SPV is more stable.

Figure 4 (row 3) presents the vertical profiles of zonal wind speed differences from the modeling results for the El Niño and La Niña phase scenarios. As can be seen, there is a strong decrease in zonal wind speed by 2 m/s in the Northern Hemisphere at 40-90 latitudes across the stratosphere during the winter months. This indicates that during the La Niña phase the SPV is quite stable and the zonal flow is quite strong, whereas during the El Niño phase the SPV is less stable. In spring months in the Northern Hemisphere at 60-90 latitudes and altitudes of 15-40 km, the zonal wind speed increases by 0.5-1 m/s, indicating that the zonal flow during the El Niño phase is stronger in spring months. The heat fluxes into the stratosphere caused by El Niño phenomena lead to increased temperature contrasts between the tropics and polar regions and between the Pacific Ocean and other regions of the Earth, and strong heating of the tropical troposphere. This contributes to enhanced ordered stratospheric heat transport, stronger meridional fluxes, and a deepening of the Aleutian Minimum, which promotes heat and mass transport from the tropics to the Arctic and warming of the Arctic stratosphere and HSP, resulting in an effect on the zonal flow, contributing to weakening of the zonal wind and SPV [41]. In the autumn months at the altitudes of 20-60 km and 30-50 latitudes in the Northern Hemisphere the zonal wind decreases by 1 m/s, while above the North Pole at the altitudes of 20-40 km the zonal wind speed increases by 0.5 m/s. In the Southern Hemisphere in the area of latitude 60 in the autumn months there is a decrease in wind speed by 0.5 m/s, but the zonal wind near the South Pole does not change much, which indicates that the SPV in the Southern Hemisphere is more stable than in the Northern Hemisphere, and that the impact on the zonal wind in the Southern Hemisphere during El Niño is weaker than in the Northern Hemisphere. As can be seen, the El Niño event and the associated stratospheric heat flux has a strong impact on the zonal wind in the Northern Hemisphere, contributing to the instability of the SPV, while in the Southern Hemisphere the SPV remains stable due to a weaker impact.

The distributions of air temperature differences, concentration and total ozone content in the stratosphere are presented below (Figure 5).

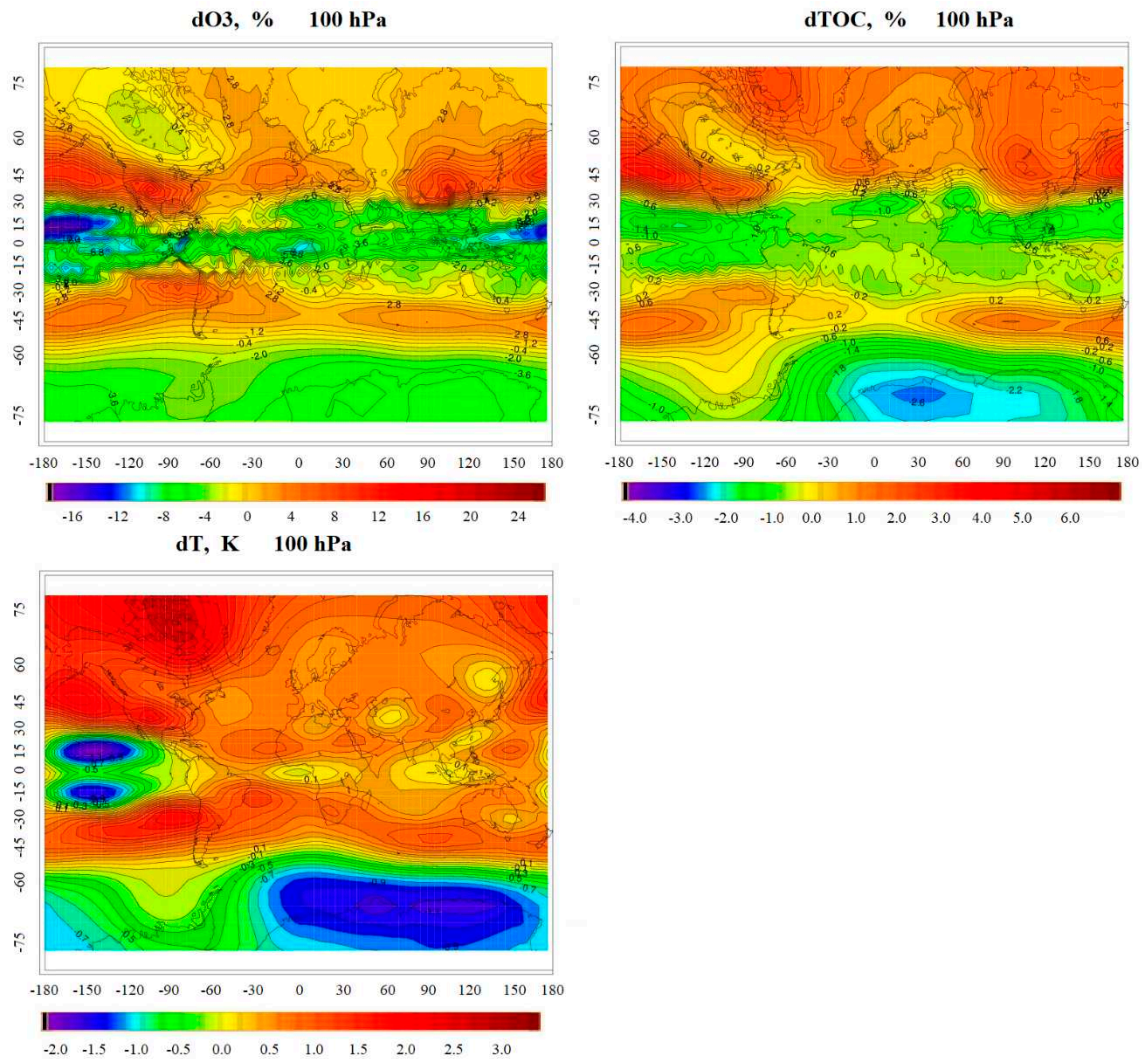


Figure 5. Distribution of the difference in ozone concentration in % at 100 hPa (low stratosphere) (top left), total ozone in % (top right), and air temperature in K at 100 hPa (bottom) based on simulation results for scenarios with El -Nino and La Nina phases.

Figure 5 shows a decrease of ozone concentration in the tropical part of the stratosphere, especially over the equatorial part of the Pacific Ocean, while an increase of ozone concentration by 3-5% is seen over the Arctic and a decrease of 3-4% over the Antarctic. The total ozone content (Figure 5, top right) shows a 1-2% decrease in ozone concentration in the tropics, especially over the Pacific Ocean in the El Niño region, which is consistent with air temperature (Figure 5, bottom) and ozone concentration in the lower stratosphere, and indicates a strengthening of the Brewer-Dobson circulation in the tropics during El Niño years. A decrease of 0.5-1% is also observed over Greenland and Antarctica, while over the Arctic there is an increase of 2% in El Niño years compared to the La Niña phase. Over Antarctica, there is a decrease of ozone content by 3% compared to the La Niña phase. Also, a 0.5% increase in ozone content is observed between Australia and Antarctica. This indicates the strengthening of the Brewer-Dobson circulation during El Niño years, which contributes to the increased transport of ozone from the tropics to the polar regions and, as a result, to the increase of ozone content over the Arctic and the decrease of ozone content in the tropics, from where it is carried to the poles. The El Niño effect is weaker in the Antarctic than in the Arctic.

Regarding stratospheric air temperature (Figure 5, bottom), a 2.5 degree decrease in air temperature is observed over the equatorial Pacific Ocean, while south of the equatorial Pacific and over much of the Arctic, the temperature increases by 1.8-2 degrees. These features may be related to enhanced stratospheric heat flux due to El Niño phenomena, which contribute to enhanced stratospheric heat flux and SSW [41], and indicate heating of the Arctic stratosphere and increased probability of SSW, which affects the zonal wind [41] and contributes to the instability of the SPV and enhanced Brewer-Dobson circulation, contributing to the transfer of heat and ozone from the tropical stratosphere to the polar stratosphere. The temperature decrease by 1-2 degrees is also observed over the Antarctic south of Australia, while over the vicinity of South America there is an increase by 0.2 degrees, indicating weak stratospheric warming in the Southern Hemisphere, and contributing to a slight weakening of the SPV and an increase of total ozone.

Figure 6 presents the vertical profiles of the differences between the meridional (top) and vertical (bottom) components of the residual circulation, based on the simulation results for the scenarios with El Niño and La Niña phases, which characterizes the changes in the heat and mass transport from the tropics to the poles.

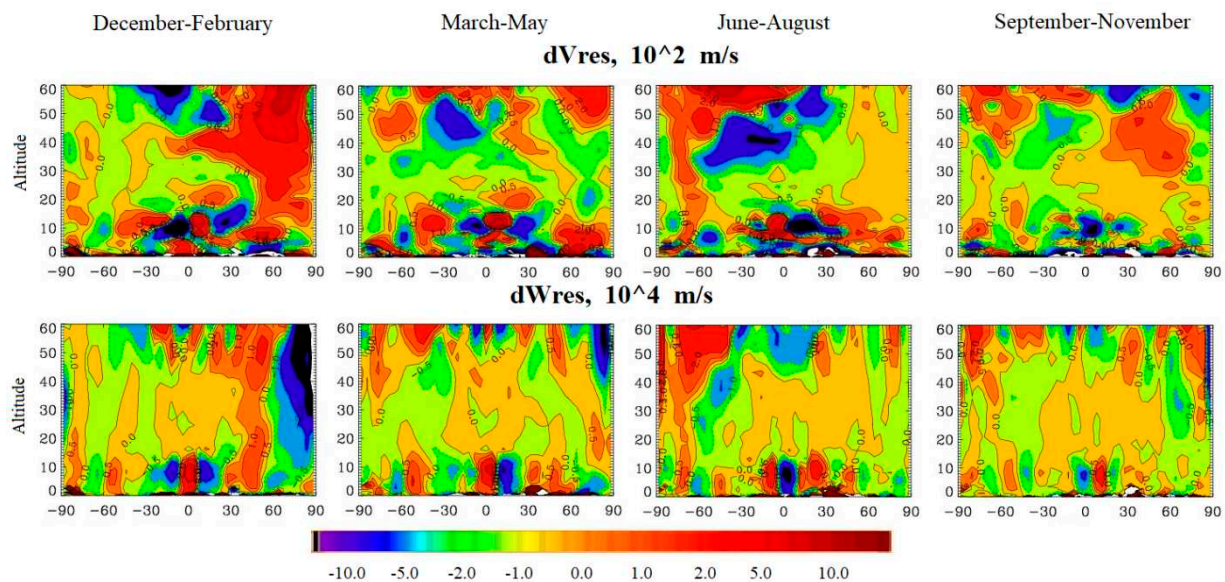


Figure 6. Vertical mean zonal mean seasonal profiles of the differences between the meridional at 10^2 m/s (top) and vertical at 10^4 m/s (bottom) components of the residual circulation based on the modeling results for the scenarios with El Niño and La Niña phases.

As can be seen, above the Arctic at the heights of 40-60 km, one observes an increase of the meridional component of the residual circulation (Fig. 6, above) by $5 \cdot 10^{-2}$ m/s at the El Niño phase in the winter months and a similar increase above the Antarctic in the summer months. At the same time, a decrease of the meridional component by $2 \cdot 10^{-2}$ m/s is observed over tropical latitudes at the same heights during the winter months. At the altitudes of 20-30 km in the Northern Hemisphere, one can observe an increase of the meridional component by $2 \cdot 10^{-2}$ m/s in the winter and autumn months, which indicates an increased transport from the equator to the North Pole. In the Southern Hemisphere at altitudes of 20-30 km, a very weak strengthening of the meridional flow by $0.5-1 \cdot 10^{-2}$ m/s in summer months is observed. As for the vertical component (Figure 5, bottom), an enhancement of $5 \cdot 10^{-4}$ m/s is observed over the equator in all months except summer months, indicating an enhancement of the vertical convective flux over equatorial latitudes due to the El Niño phenomenon.

Also in the winter months, a decrease of the vertical component by $5 \cdot 10^{-4}$ m/s is observed above the Arctic at the heights of 20-60 km. These changes in the components of the residual circulation indicate an intensification of the Brewer-Dobson circulation during the El Niño phase, and, as a result, ozone supply from tropical latitudes to the Arctic latitudes. El Niño leads to air heating in the tropical

region, which contributes to the intensification of temperature contrasts and, as a result, to the intensification of convective flows in the tropical troposphere and deepening of the Aleutian Minimum. All this enhances the orderly heat transfer from the troposphere to the stratosphere. These flows contribute to stratospheric heating and SSW, which contributes to the strengthening of the meridional flow, which affects the zonal flow, contributing to its weakening and circulation, as a result of which the SSW loses stability and becomes weaker [41]. These processes contribute to the strengthening of the Brewer-Ra-Dobson circulation, resulting in an increase in the heat and ozone transport from the tropical part of the stratosphere to the Arctic stratosphere. As a result, the air temperature and ozone concentration increases in the Arctic stratosphere, while in the tropical stratosphere it decreases. In the Southern Hemisphere, this effect is much weaker, the heat and ozone transport is less intense than in the Northern Hemisphere, therefore the zonal flux and SPV and hence the ozone holes over the Antarctic are more powerful and stable than over the Arctic.

Below are the differences in the components and divergence of the flux of Plumb wave activity based on the modeling results for scenarios with the El Niño phase and the La Niña phase, which characterizes the transfer of heat and mass due to waves (Figure 7).

As can be seen, over the Northern Hemisphere, there is a strong amplification of the zonal component of the Plumba flux at altitudes 30-60 km by $10 \text{ m}^2 \text{ s}^{-2}$ and the vertical component of the Plumba flux by $2.5 \cdot 10^{-2} \text{ m}^2 \text{ s}^{-2}$ at altitudes 20-60 km in winter and fall months. The meridional component has a decrease of $10 \text{ m}^2 \text{ s}^{-2}$ at altitudes 30-60 and an enhancement of $0.5 \text{ m}^2 \text{ s}^{-2}$ at altitudes 10-30 km. At altitudes of 0-30 km and 30-60 latitudes in winter months, a decrease of the zonal component by $1 \text{ m}^2 \text{ s}^{-2}$ and strengthening of the meridional component of the Plumb flow by $0.5 \text{ m}^2 \text{ s}^{-2}$ are observed. Strengthening of the meridional and vertical components at the altitudes of 20-30 km is related to the strengthening of meridional processes due to stratospheric heating, which contribute to the weakening of the zonal flux and Rossby waves. This amplification indicates an increase in the intensity of propagation of planetary Rossby waves from the troposphere to the stratosphere due to enhanced heat fluxes from the stratosphere during the Southern Oscillation. These heat fluxes contribute to the enhanced wave activity flux from the tropics to the pole and from the troposphere to the stratosphere, which contributes to the instability of Rossby waves. All of this affects the zonal wind and disrupts the SPV, resulting in enhanced Brewer-Dobson circulation and heat and ozone transport from the tropics to the polar regions. As for the Southern Hemisphere, at the altitudes of 40-60 km, one observes an intensification of the zonal component of the Plumb flow in the spring and autumn months by $0.5 \text{ m}^2 \text{ s}^{-2}$. In the summer months, an increase of $5 \text{ m}^2 \text{ s}^{-2}$ is observed at altitudes 0-30 km. The meridional component shows an increase by $0.5 \text{ m}^2 \text{ s}^{-2}$ in the spring and fall months and by $5 \text{ m}^2 \text{ s}^{-2}$ in the summer months at altitudes of 20-50 km, indicating an increase in the meridional flow of wave activity from the equator to the South Pole. The vertical component shows an increase of $0.5 \cdot 10^{-2} \text{ m}^2 \text{ s}^{-2}$ during spring and fall months at altitudes of 20-60 km and $2 \cdot 10^{-2} \text{ m}^2 \text{ s}^{-2}$ during summer months at altitudes of 30-60 km. These phenomena indicate the strengthening of the wave activity flux in the Northern Hemisphere and weakening of this flux in the Southern Hemisphere, which, in turn, contributes to the weakening of planetary Rossby waves and the destruction of the SPV, especially in the Northern Hemisphere, and the transfer of heat by planetary waves from the equator to the pole and from the troposphere to the stratosphere.

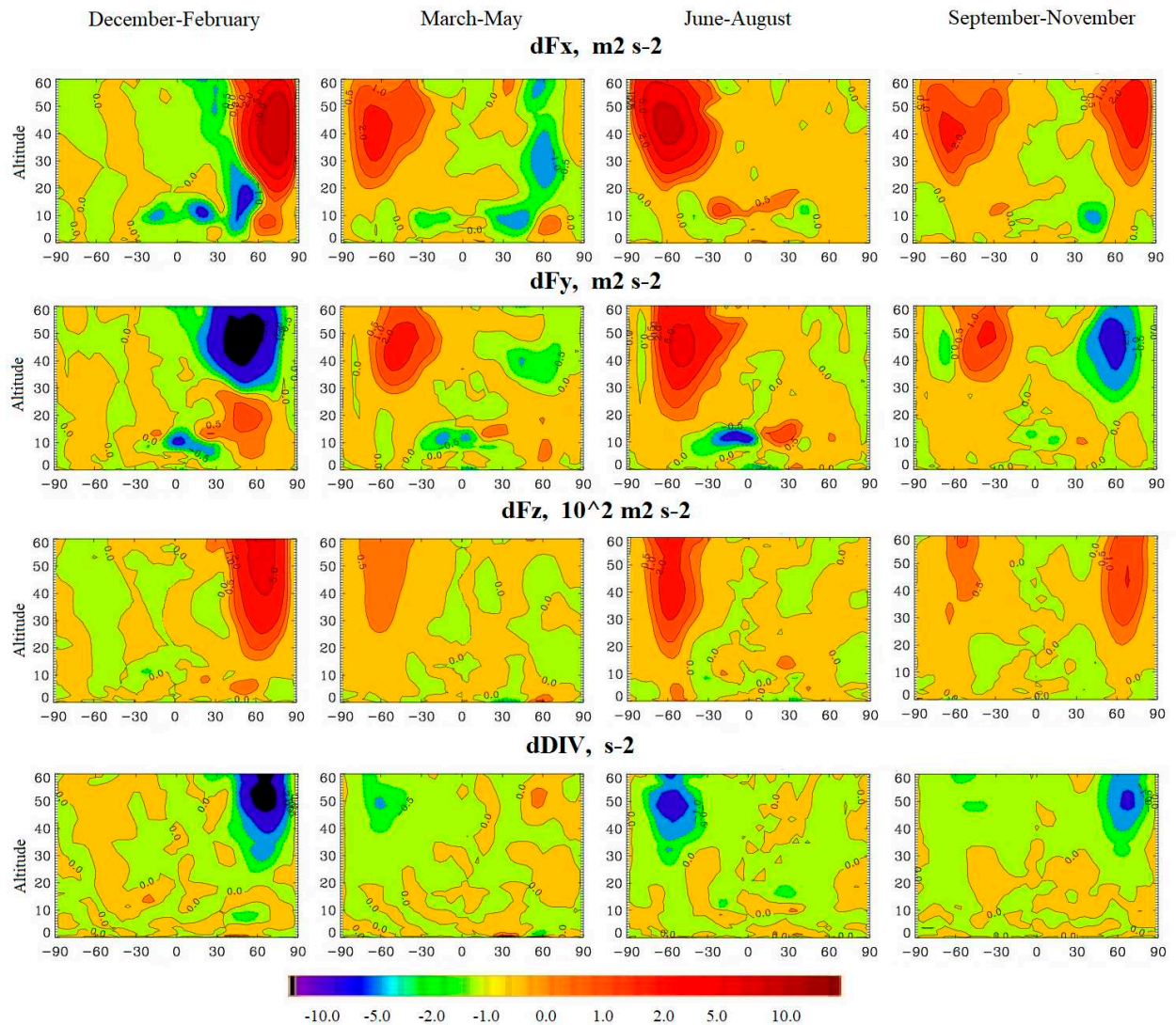


Figure 7. Vertical zonal mean seasonal mean profiles of differences of zonal (1 row), meridional (2 row) (in $\text{m}^2 \text{s}^{-2}$), vertical (3 row) (in $10^2 \text{m}^2 \text{s}^{-2}$) and divergence (in s^{-2}) (4 row) components of the residual circulation based on the modeling results for the scenarios with El Niño and La Niña phases.

As for the divergence of the wave activity flux (Figure 7, row 4), there is a negative anomaly between El Niño and La Niña phases in the Northern Hemisphere at 30-60 km altitudes in the winter and fall months of $2-5 \text{ s}^{-2}$, and weaker (up to 0.5 s^{-2}) in the spring months. In the Southern Hemisphere, there is a weak negative divergence anomaly in the spring and summer months (up to 2 s^{-2}) at altitudes of 40-60 km. This means that during the El Niño phase there are more dramatic changes in the flow of wave activity in the Northern Hemisphere than during the La Niña phase. El Niño contributes to the enhancement of the meridional and vertical flux of wave activity into the stratosphere. This contributes to the enhanced convergence of the Plumb flow, as indicated by the negative anomalies, and hence to the reversal of the zonal flow and weakening of the Rossby waves. These changes are related to the enhanced heat flux into the stratosphere during the El Niño phase, which contributes to the enhanced meridional temperature transport from the tropics to the polar regions, which affects the zonal wind, and contributes to the enhanced wave activity flux. This both weakens the planetary Rossby waves during the El Niño phase and enhances the propagation of heat into the stratosphere through these waves, which contributes to the destruction of the SPV and SSW. In the Southern Hemisphere, this influence is much weaker than in the Northern Hemisphere.

Also, to analyze the wave activity, the amplitude differences of planetary waves with wave numbers 1 and 2 were calculated from the experimental results for the El Niño phase and La Niña phase scenarios presented in Figure 8.

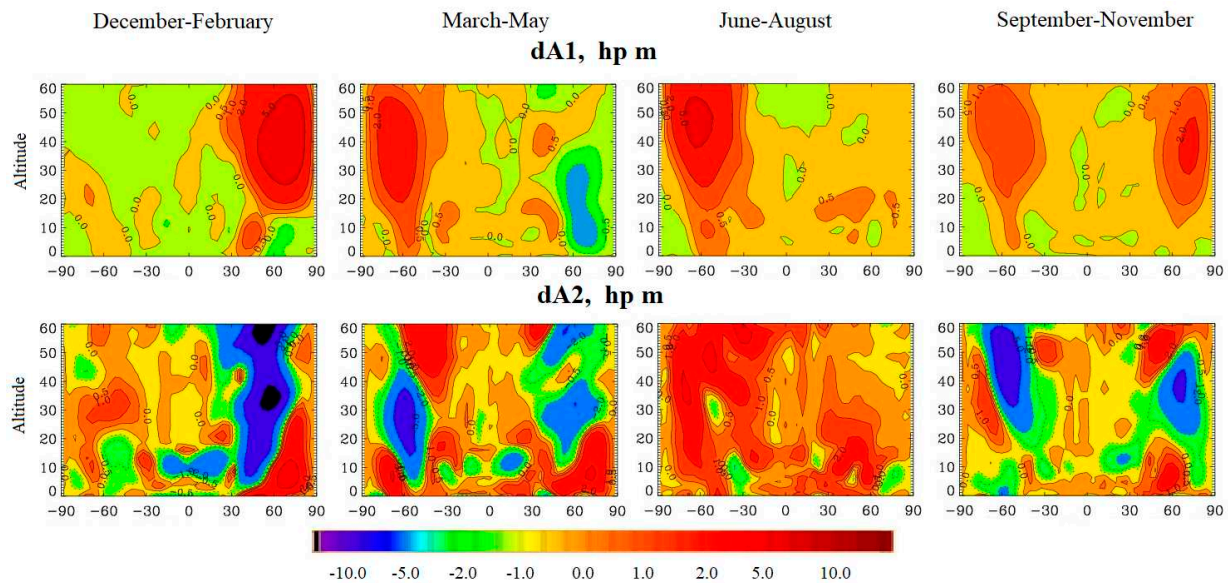


Figure 8. Vertical zonally mean seasonally mean profiles of the differences between the wave amplitude with wave number 1 in hp m (top) and the wave amplitude with wave number 2 in hp m (bottom) from modeling results for scenarios with El Niño and La Niña phases.

As can be seen from the figure, in the Arctic stratosphere (60-90 latitudes, heights from 15 km) in the winter months there is an increase in the amplitude of this wave by 5 hp m. In the spring months, there is a decrease in amplitude at altitudes of 20-30 km by 1 hp m. During the summer months, the amplitude of the wave with number 1 in the Arctic increases by 0.5 hp m. In the fall months, this amplitude increases by 2 hp m throughout the Northern Hemisphere at altitudes of 15 km or more. As for the amplitude of the wave number 2 (Figure 7, bottom), in the Northern Hemisphere at 30-60 latitudes, there are two centers of amplitude decrease by 2-5 gp m at altitudes of 10-30 km and at altitudes of 45-60 km in winter months, and amplitude increase by 2 gp m at 5-30 km. During the spring months, there is an increase in wave number 2 amplitude by 2 gp m at altitudes 5-30 km, and a decrease of 10 gp m at altitudes 25-60 km and 30-60 latitudes. In the summer months, the amplitude of the wave with number 2 increases by 2 hp m at the altitudes of 5-40 km near latitude 60, and in the autumn months in this place, but up to the altitude of 20 km, the amplitude increases by 1 hp m. At the same time in the autumn months one can also see a center of amplitude decrease by 2 hp m at the altitudes of 30-40 km. The increase in the amplitude of the wave with number 1 and decrease in the amplitude of the wave with number 2 in the Northern Hemisphere in winter and partly in spring and autumn months is connected with the increased heat flux to the stratosphere due to El Niño.

This heat flux leads to stratospheric heating and intensification of meridional processes, which lead to an intensification of the wave activity flux. As a result, there is an increase in the amplitude of the wave amplitude with number 1, and weakening of the amplitude of the wave amplitude with number 2, which contributes to the amplification of the wave activity flux that destroys the SPV, which leads to an increase in the Brewer-Dobson circulation and increases the air temperature and ozone content in the Arctic stratosphere. As for the Southern Hemisphere, the largest increases in the amplitudes of the number 1 wave are observed during the spring and summer months (by 2-5 hp m over the entire thickness of the Southern Hemisphere stratosphere), whereas during the fall months the amplitude of the number 1 wave increases by only 1 hp m. The amplitude of the wave with number 2 in the Southern Hemisphere decreases only in the spring and autumn months by 2 hp m

in the region of latitude 60 at the altitudes of 15-40 km, whereas in the summer months it increases by 5 hp m over the entire stratospheric thickness. Thus, in the Southern Hemisphere, the effect associated with the Southern Oscillation is mainly manifested in the wave amplitude with number 1, indicating a weaker enhancement of the wave activity flux compared to the Northern Hemisphere. This is because the zonal wind is stronger in the Southern Hemisphere than in the Northern Hemisphere and therefore the SPV is more stable. Thus, the Southern Oscillation has a significant effect on planetary waves and wave activity in the Northern Hemisphere, and a weaker effect on waves and wave activity in the Southern Hemisphere.

3.3. Influence of the long-term SST trend on stratospheric processes

In this study, numerical experiments were carried out using simulation results from SST data for the conditions of the beginning of the period (early 1980s) and the end of the period (late 2010s). At the same time, as in the case of ENSO, the remaining factors were fixed at the level of 2020, which makes it possible to conduct a pure experiment to assess the influence of the SST trend on the structure and composition of the atmosphere.

Figure 9 (row 1) presents vertical profiles of air temperature differences between the modeling results for the end and beginning of the trend scenarios. As can be seen, a warming of 0.2-0.5 degrees is observed in the troposphere for all seasons. This confirms the warming of the troposphere that is occurring throughout the globe (global warming). In the stratosphere in the tropics, air temperature varies little throughout the year. Also, in the winter months there is a warming of 0.5-1 degrees in the Arctic stratosphere at altitudes of 30-60 km and in the spring by 2 degrees at altitudes of 20-40 km, which may be associated with an increase in heat flows into the stratosphere, a deepening of the Aleutian minimum and an increase in the probability of SSWs due to ocean warming. These heat fluxes influence the zonal wind and SPV, which contributes to the strengthening of the Brewer-Dobson circulation and warming of the Arctic stratosphere. At the same time, in winter there is also a decrease in temperature by 0.5 degrees at altitudes of 10-30 km. In spring and autumn at these altitudes there is a decrease in temperature of 1 degree. In the Southern Hemisphere, in the stratosphere there is a decrease in temperature by 0.5-1 degrees in the winter and autumn months at altitudes of 10-30 km, while in the summer and spring months there is an increase in temperature by 0.5 degrees at altitudes of 20-40 km and by 1 degree at altitudes 40-50 km, indicating a weaker increase in heat fluxes and the Brewer-Dobson circulation towards the South Pole compared to the Northern Hemisphere. This confirms the fact that the SST trend has less impact on stratospheric processes than ENSO.

Figure 9 (2nd row) shows the vertical profiles of the differences in ozone concentration between the modeling results for the end and beginning of the trend scenarios. Vertical profiles show that ozone concentration increases in the tropical troposphere by 2-5% in all seasons, and in the Arctic stratosphere by 2% at altitudes up to 10-30 km throughout the year due to heating of the stratosphere by vertical flows associated with ocean warming.

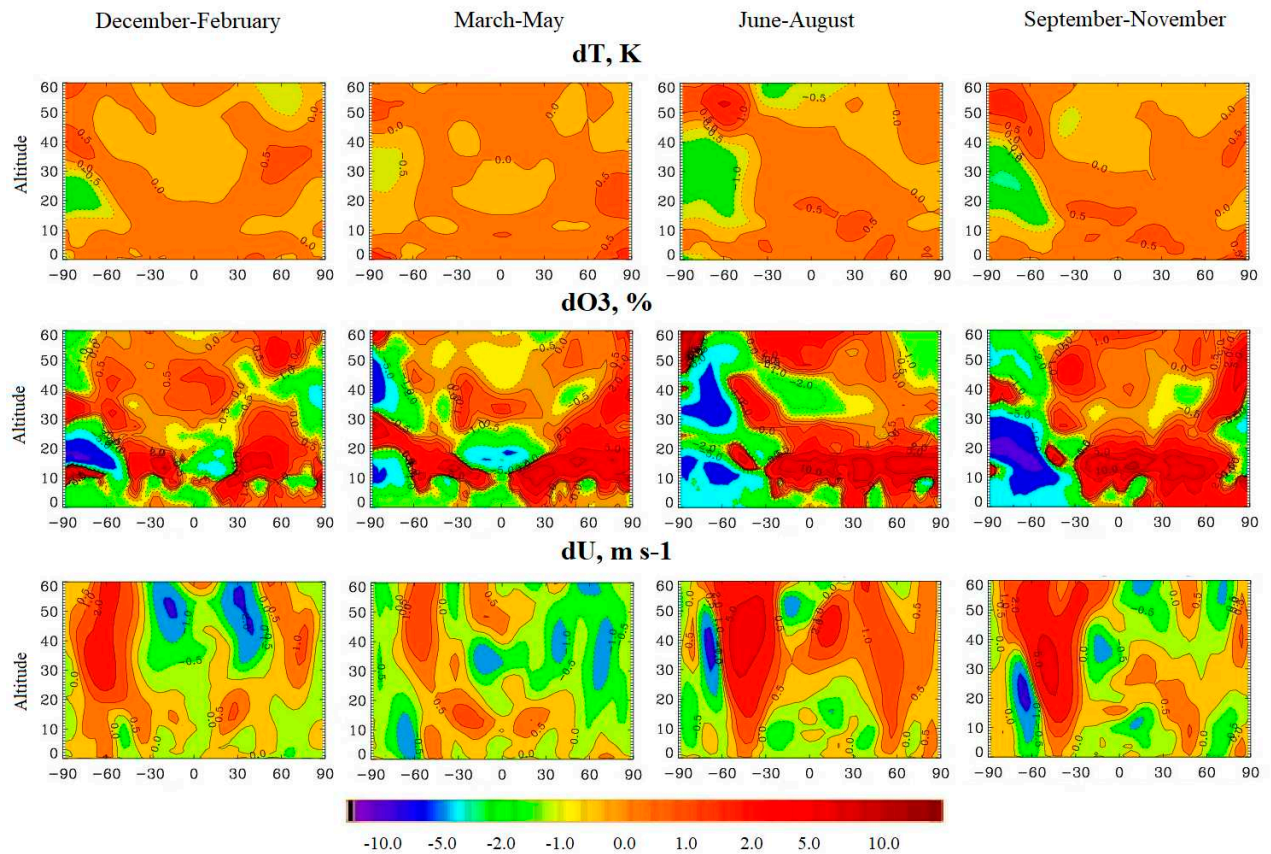


Figure 9. Vertical zonal mean seasonal profiles of air temperature differences (1st row), ozone concentration (2nd row) and zonal wind speed in m/s (3rd row) based on modeling results for the scenarios of the late 2010s and early 1980s.

At the same time, during winter, spring and fall months, a decrease in ozone concentration over the Arctic by 1-2% at altitudes of 20-40 km is observed. These flows have an impact on the zonal wind, contributing to its weakening and weakening of the SPV. As a result, the meridional transport and the Brewer-Dobson circulation, which transports temperature and ozone from the tropics to the poles, may be enhanced. Thus, warming of the troposphere contributes to the increase of ozone concentration in the tropics and over the Arctic, which can be a sign of the Bruer-Dobson circulation strengthening and the increase of heat fluxes to the Arctic stratosphere. But this effect is weaker than in the case of ENSO. At the same time over the Antarctic, the ozone concentration decreases by 0.5-1% at altitudes up to 20-30 km in winter and autumn months, and increases by 1-5% in summer and, especially, spring months, which can be connected with the influence of seasonal changes of ozone concentration in spring months and with weaker compared to the Northern Hemisphere heat fluxes and strengthening of the Brewer-Dobson circulation, due to which the strong zonal flux and the SPV remain very stable, which contributes to the air temperature decrease in the Antarctic stratosphere and favors the chemical processes in the Antarctic stratosphere with participation of bromine and chlorine. That is, the SST increase due to the multiyear trend contributes to deepening of the ozone hole in the Antarctic. Compared to ENSO, the influence of the trend on the ozone concentration is weaker and is manifested mainly in the in the Northern Hemisphere.

Figure 9 (3rd row) presents the vertical profiles of the differences in zonal wind speed between the simulation results for the end and beginning of the trend scenarios. As can be seen, there is an increase in the zonal flow over the Arctic during the year by 2 m/s, while in the summer months it weakens, as can be seen from the anomalies of the zonal wind speed of 0.5 m/s over the Arctic. Moreover, in the autumn months, at altitudes of 10-30 km near the pole, a reversal of the zonal wind is observed, which is evident from the negative anomaly of 0.5-1 m/s. At the same time, over Antarctica there is an increase in the zonal flow by 1 m/s throughout the year. This may be due to the

fact that warming of the ocean, and therefore the troposphere, has a greater impact on the Arctic than on the Antarctic due to the geographic configuration of the Arctic (sea surrounded by land) and Antarctica (land surrounded by sea). That is, “Arctic amplification” is manifested - strong warming of the Arctic and increased heat flows into the stratosphere due to an increase in SST and air temperature in the Arctic troposphere, affecting the zonal wind. Warming of the troposphere contributes to a slight weakening of the zonal flow in the Northern Hemisphere, and an increase in the meridional flow, and may also contribute to SSW. The SSW in 2019 could also have an impact on the zonal flow. This could strengthen the Brewer-Dobson circulation, contributing to higher air temperatures and ozone levels in the Arctic stratosphere. At the same time, the effect of the SST trend on the zonal wind is much weaker compared to ENSO. In the Southern Hemisphere, the zonal flow is generally increasing, indicating its stability and the absence of any powerful heat flows into the Antarctic stratosphere, which could weaken the zonal wind and strengthen the Brewer-Dobson circulation, which may also be associated with a decrease in SST and air temperatures in Antarctica. The weakening of the zonal flux due to an increase in SST is less than that due to short-period SST fluctuations, and is manifested only in the Arctic stratosphere.

The distributions of air temperature differences, ozone concentration and total ozone content in the stratosphere are presented below (Figure 10). These figures show an increase of ozone concentration and total ozone content by 1-3% over the tropical Pacific Ocean and by 0.5% in the Arctic stratosphere, and a decrease by 3-5% in the Antarctic stratosphere. We also see a 1-3% decrease in ozone concentration and total ozone content over the tropical Atlantic and over Siberia. The distribution of ozone differences is consistent with stratospheric air temperature (Figure 10, bottom). Decreases in ozone concentration and content are observed mainly in the Southern Hemisphere over the Atlantic. In the Northern Hemisphere, ozone content increases, except in Siberia. The decrease in ozone in the tropics and increase in the Northern Hemisphere indicates an enhanced Brewer-Dobson circulation, which transports air temperature and ozone from the tropics to the poles, but this effect is much smaller than in the case of ENSO. In the Southern Hemisphere, the ozone transport to the Southern Hemisphere is practically absent, due to which the ozone content decreases.

As for the air temperature in the stratosphere (Figure 9, bottom), a warming of 1-2 degrees is observed over the tropics, especially over the Pacific Ocean and Australia, and a warming of 1 degree over the Canadian Arctic. Also in the stratosphere there is a decrease in temperature in the Southern Hemisphere by 0.5-1.0 degrees, and over the Arctic in the region of Chukotka and Alaska - by 1-2 degrees. The increase in temperature over the Atlantic and North America is due to increased heat fluxes from the troposphere and SSW. SST changes have a much smaller effect on the stratosphere than on the troposphere, but, nevertheless, the ocean still affects it indirectly. Compared to ENSO, the influence of the SST trend on the stratosphere is less significant. However, an increase in SST still contributes to increased heat fluxes into the stratosphere, as can be seen from the increase in air temperature in the Northern Hemisphere. In the Southern Hemisphere, air temperatures are decreasing, indicating a weakening of heat fluxes into the stratosphere over Antarctica, and an increase in zonal flux.

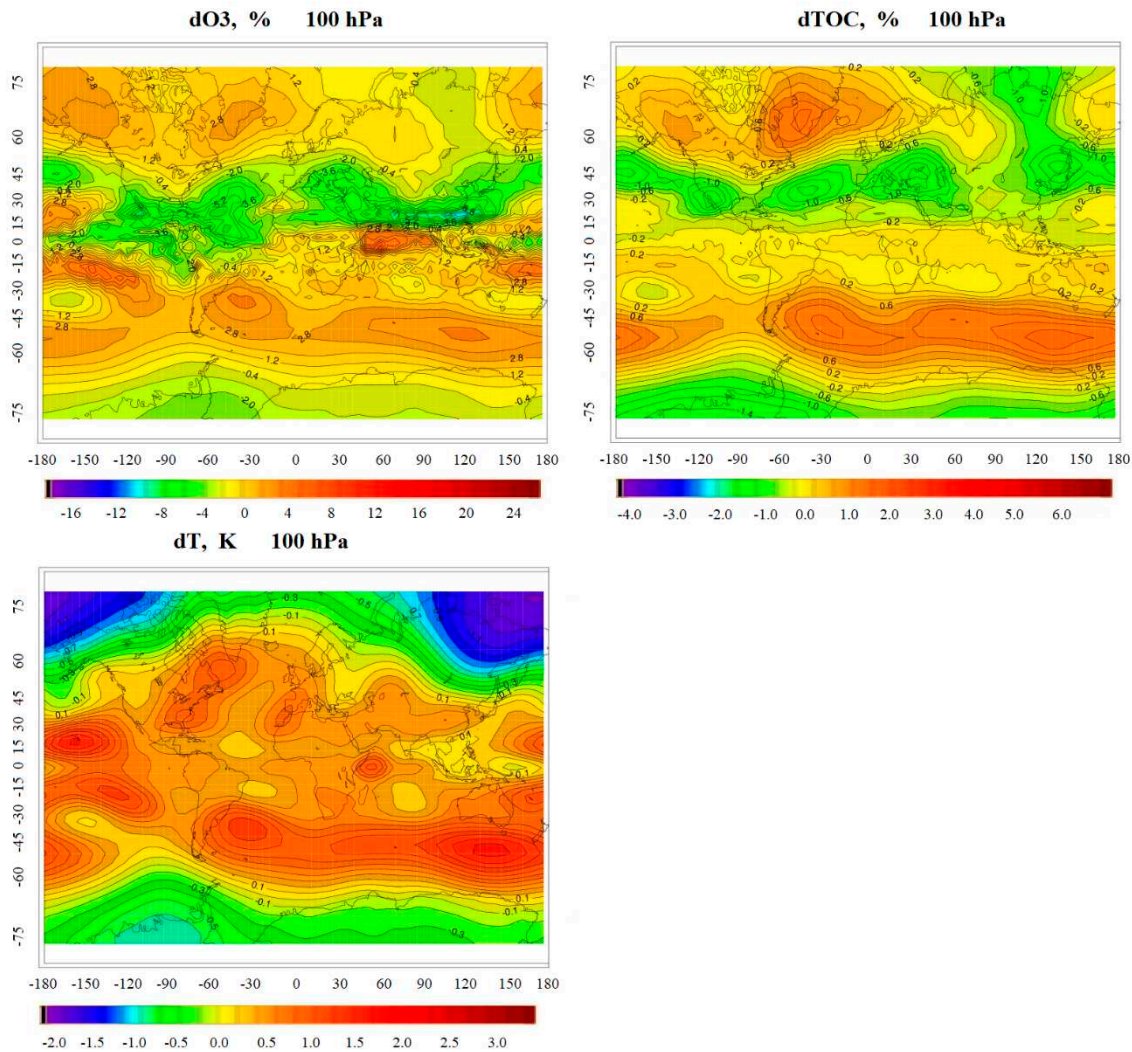


Figure 10. Distribution of the difference in ozone concentration in % at 100 hPa (low stratosphere) altitude (top left), total ozone in % (top right), and air temperature in K at 100 hPa altitude (bottom) based on simulation results for scenarios of the end of 2010- x and early 1980s.

Figure 11 presents the vertical profiles of the differences of the meridional (top) and vertical (bottom) components of the residual circulation between the modeling results for the end and the beginning of the trend scenarios. As can be seen, there is an increase of the meridional component above the equator by $2 \cdot 10^{-2}$ m/s at the altitudes of 10-15 km, and an increase in the Northern Hemisphere in the spring and autumn months by $1-2 \cdot 10^{-2}$ m/s. At the same time in winter months there is a decrease by $1-2 \cdot 10^{-2}$ m/s, indicating a weaker strengthening of meridional transport from the tropics to the Northern Hemisphere compared to ENSO. In the vertical component, an increase of $2 \cdot 10^{-4}$ m/s in the tropical part of the troposphere and a decrease of $2 \cdot 10^{-4}$ m/s in the equatorial part of the troposphere are observed, indicating an enhanced heat flux to the stratosphere in the tropics and a weakening at the equator. There is also an increase in vertical flux by $2 \cdot 10^{-4}$ m/s. This means that ocean and lower troposphere warming in the Northern Hemisphere due to "Arctic amplification" and general warming of the lower troposphere may contribute to enhanced heat fluxes into the Arctic stratosphere, resulting in stratospheric heating and SSWs that affect zonal wind and SPV in the Northern Hemisphere. As a result, the meridional transport of air masses from the tropical region to the Arctic region is enhanced. This contributes to the strengthening of the Brewer-Dobson circulation from the tropics to the North Pole due to the increase of the SST and, hence, to the warming of the Arctic stratosphere and increase of the ozone content in the Northern Hemisphere. In the Southern Hemisphere, the effect is practically absent as there is a decrease of SST and air temperatures in the

troposphere, and the meridional transport from the tropics to the South Pole is insignificant. As a result, the zonal flux and SPV are stable, the air temperature decreases and the ozone content decreases due to chemical processes involving chlorine and bromine.

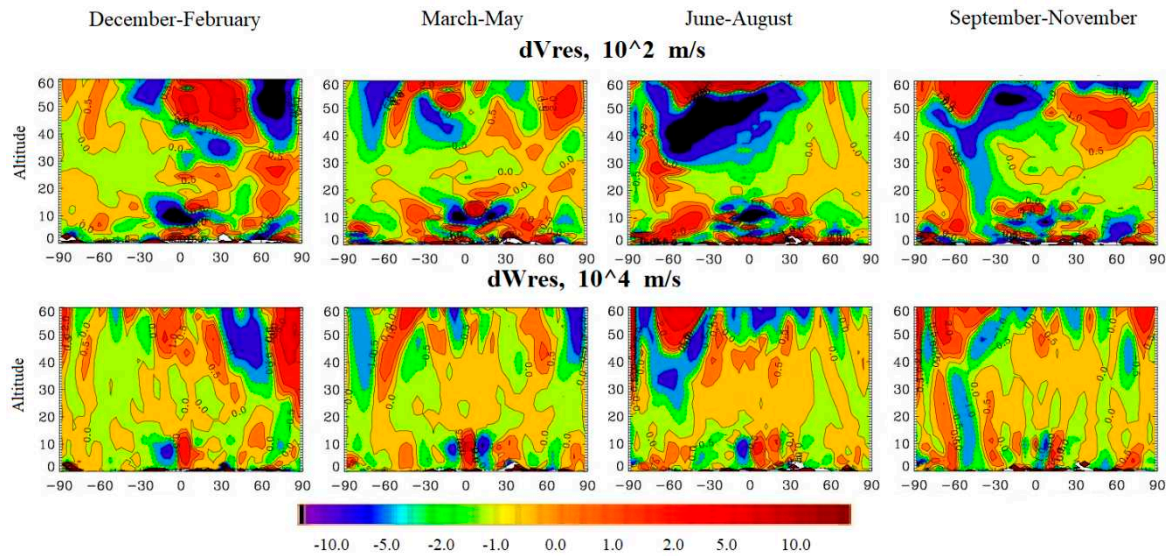


Figure 11. Vertical mean zonal mean seasonal profiles of the differences between the meridional at 10^2 m/s (top) and vertical at 10^4 m/s (bottom) components of the residual circulation based on the modeling results for the scenarios of the late 2010s and early 1980s.

The vertical profiles of the differences in the zonal (Figure 11, 1st row), meridional (Figure 11, 2nd row) and vertical (Figure 11, 3rd row) components and the divergence (Figure 11, 4th row) of the Plumb wave activity flux between the modeling results for the end-of-trend and beginning-of-trend scenarios are presented below.

As can be seen, there is a decrease of $5\text{--}10\text{ m}^2\text{ s}^{-2}$ in the zonal component over the Arctic at altitudes 20–50 km during winter months and at altitudes 30–60 km at latitude 60 during fall months, and an increase of $1\text{ m}^2\text{ s}^{-2}$ at altitudes 10–30 km during winter and spring months, and at altitudes 40–60 km during fall months. The meridional component increases by $2\text{--}10\text{ m}^2\text{ s}^{-2}$ at latitudes 30–90 degrees and altitudes 10–50 km during winter and fall months, and decreases by $1\text{ m}^2\text{ s}^{-2}$ at altitudes 10–20 km during winter months. The vertical component decreases by $2\text{--}5 \times 10^{-2}\text{ m}^2\text{ s}^{-2}$ around latitude 60 at altitudes 30–60 km during the winter months. We also see an increase in divergence by 2 s^{-2} at altitudes 40–60 km during the winter months. These changes indicate a slight strengthening of the wave activity flux from the tropics to the North Pole and to the Arctic stratosphere due to the "Arctic amplification", which may contribute to the heat transport to the Arctic stratosphere, and, as a consequence, weakening the zonal flux and destroying the SPV, contributing to the strengthening of the Brewer-Dobson circulation and increasing the ozone content.

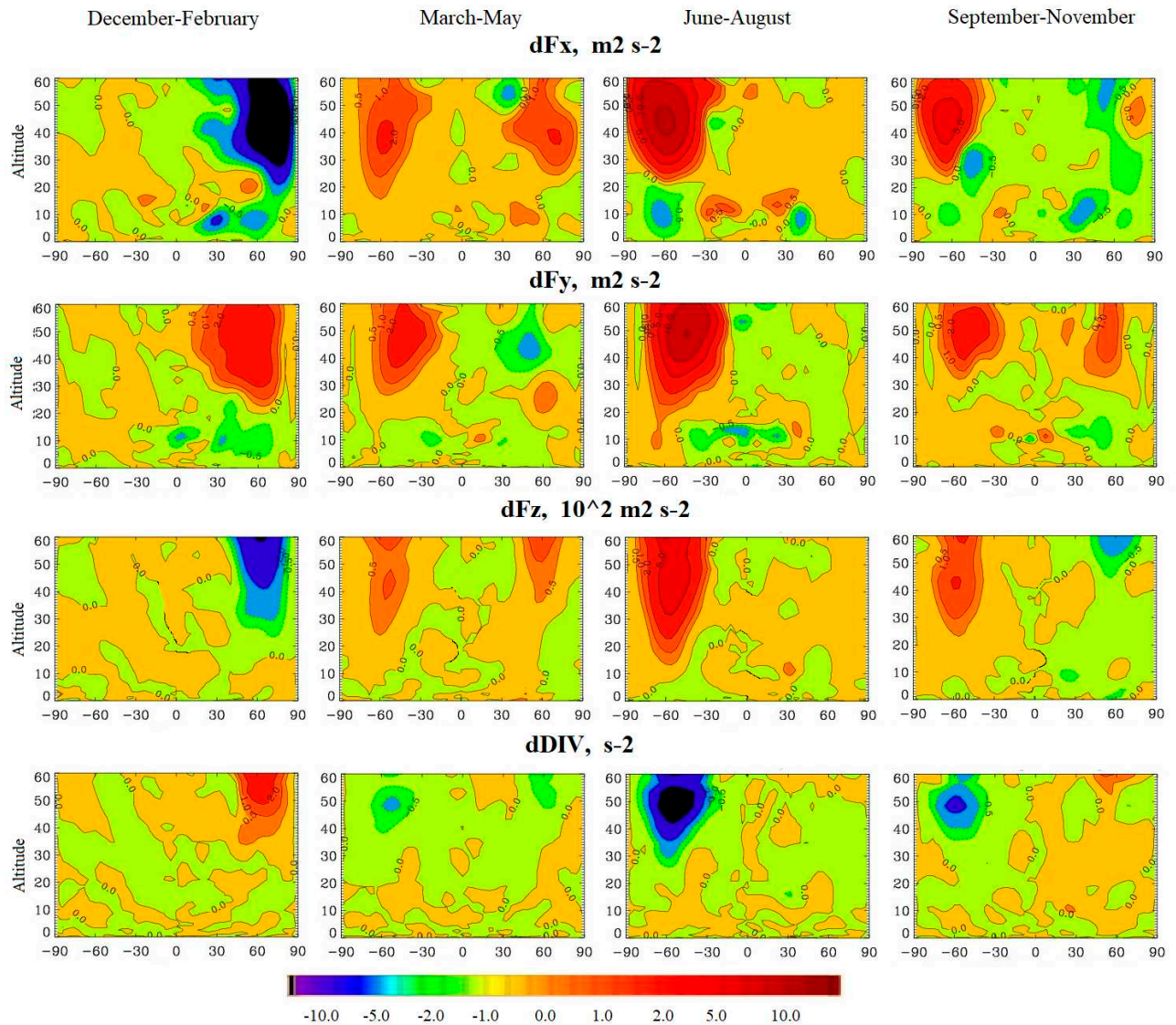


Figure 12. Vertical zonal mean seasonal profiles of differences of zonal (1 row), meridional (2 row) (in $\text{m}^2 \text{s}^{-2}$), vertical (3 row) (in $10^2 \text{m}^2 \text{s}^{-2}$) and divergence (in s^{-2}) (4 row) components of the residual circulation based on modeling results for the scenarios of the late 2010s and early 1980s.

Above the Antarctic, one observes an increase by $10 \text{ m}^2 \text{s}^{-2}$ at 30-60 km heights in the summer months of the zonal component; an increase by $2\text{-}5 \text{ m}^2 \text{s}^{-2}$ at 30-60 km heights in the summer and autumn months of the meridional component and an increase by $2 \times 10^{-2} \text{ m}^2 \text{s}^{-2}$ in summer of the vertical component. At the same time, there are no significant amplifications of the wave activity flux components at the altitudes of 20-30 km. One can also see an increase in the con-vergence by 5 s^{-2} in summer and fall months at altitudes of 40-60 km. This indicates that there is no heat transfer from the troposphere to the Antarctic stratosphere in the Southern Hemisphere due to the decreased SST and air temperature in the Antarctic. Therefore, the zonal flux and SPV are stable, the Brewer-Dobson circulation is not intensified and the ozone content is decreased. In contrast to ENSO, the ocean warming due to the trend has a smaller impact on the wave activity flux. But the positive anomalies of the meridional component in the Arctic stratosphere indicate an intensification of this component, which contributes to the instability of the planetary Rossby waves, and to the weakening of zonal transport and destruction of the SPV.

Figure 13 shows the differences in the amplitudes of planetary waves with wave number 1 (top) and wave number 2 (bottom) according to the experimental results for the end and beginning of the trend scenarios.

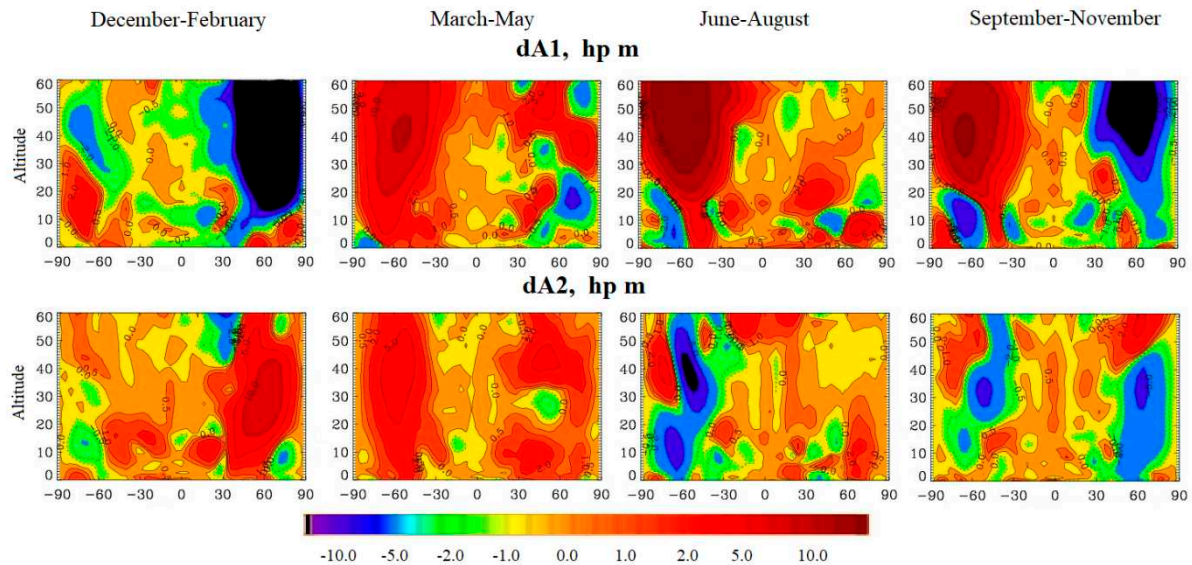


Figure 13. Vertical zonal mean seasonal profiles of the differences between wave amplitude with wave number 1 in hp m (top) and wave amplitude with wave number 2 in hp m (bottom) from modeling results for the late 2010s and early 1980s scenarios.

As can be seen from the figure, in the Arctic stratosphere in the winter months at altitudes 20-60 km there is a decrease in the amplitude of the wave number 1 by 5-10 hp m at altitudes 20-60 km. During the spring months, a decrease of 2 hp m in amplitude is observed at 10-20 km and 50-60 km altitudes in the Arctic, with a 0.5-1.0 hp m increase in amplitude at 30-45 km altitudes. During the summer months, the amplitude in the Arctic does not change much. During the fall months, there is a decrease of 5 hp m in amplitude at altitudes of 20-60 km in the Northern Hemisphere. Regarding the amplitude of the wave number 2 (Figure 12, bottom), an increase of 10 hp m in amplitude is observed at altitudes of 5-50 km over the Arctic during the winter months. In the spring months, a 5 hp m increase in amplitude is observed at altitudes 5-60. During the fall months, the amplitude of the wave number 2 decreases by 5 hp m throughout the Northern Hemisphere. The decrease in the amplitude of the number 1 wave and increase in the amplitude of the number 2 wave during the winter months in the Northern Hemisphere indicates very little or no enhancement of the heat flux due to the upward trend of the SST and the "Arctic Boost" that contribute to the meridional flux and wave activity flux that inhibits zonal wind and destroys the SPV. However, the effect associated with the SST trend is very weak compared to the effect of the Southern Oscillation. As a result, the Brewer-Dobson circulation is practically not enhanced and the air temperature and ozone content in the stratosphere of the Northern Hemisphere do not change much.

As for the Southern Hemisphere, in the winter months at altitudes of 30-50 km, the amplitude of the wave number 1 decreases by 0.5-1 hp m, while at 10-30 km it increases by 2 hp m. In the spring, summer and autumn months at the altitudes of 20-60 km, the amplitude increases by 5-10 hp m. The amplitude of the wave with number 2 decreases in the autumn months by 1 hp m in the region of latitude 60 and altitudes of 20-40 km, and in the summer months - by 5 hp m throughout the stratosphere. In the spring months, the amplitude of the wave number 2 increases by 5 hp m over the entire stratosphere. Thus, in the Southern Hemisphere, the effect associated with the SST trend is manifested in a decrease in the amplitude of the wave with number 2 in the summer and fall months and an increase in the amplitude of the wave with number 1. The increase in the amplitude of the wave with number 1 indicates an increase in the flux of wave activity in the Southern Hemisphere due to the influence of the SST trend. However, analysis of air temperature, ozone concentration and zonal wind (Figures 8-10) indicate a steady SPV and decreasing ozone concentration in the Southern Hemisphere. This indicates a very weak effect on the zonal wind and the persistent SPV, leading to

a deepening of the ozone hole in the Southern Hemisphere. Thus, the SST trend has an impact on the planetary waves and wave activity only in the Northern Hemisphere.

4. Discussion

Based on the results of numerical experiments with CCM, the response of the stratosphere of the Northern and Southern Hemispheres to ENYUK and to the multiyear trend of the SST increase is studied. In addition, taking into account previous results [60,61], the coupling and response of ENJC in the mid- and high-latitude stratosphere is analyzed for the Northern and Southern Hemispheres. Our study complements previous studies [21,28,60] showing a weakening of the ENYUK-related SPV and the heterogeneity of the Northern and Southern Hemisphere SPV response to ENYUK during the cold half of the year [62].

It has been shown that a weakening of SPV in the Arctic is observed in the stratosphere in response to the El Niño phase in the winter months, while in the Antarctic - in the autumn [60]. This weakening may be associated with SSW due to El Niño. The MERRA2 reanalysis data confirms the simulation results. The destruction of the SPV during El Niño is primarily associated with the SSW. Previous studies [21,33,34] have shown an increase in the probability and number of SSWs during the winter months during the El Niño phase, while the relationship with the La Niña phase is ambiguous. The modeling results show that during the La Niña phase there are practically no SSWs, and the SPV is more stable than during the El Niño phase. However, in reality, during La Niña there are also SSWs. This depends, first of all, on the type of La Niña (eastern or central type), as well as on factors independent of ENSO [60].

Regarding stratospheric ozone, previous studies have mainly investigated the influence of ENSO on the dynamic and thermal processes in the stratosphere, and little attention has been paid to the remote coupling and the effect on ozone. This study shows that ozone concentration and total ozone content increase during the El Niño phase in winter months, which confirms the findings of [12]. The increase in ozone concentration is primarily due to the strengthening of the Brewer-Dobson circulation, resulting in an increase in ozone influx into the polar stratosphere. During the La Niña phase due to the stable SPV and absence of the SSW according to the modeling results, the concentration and total ozone content in the polar stratosphere decrease, which is connected with the weak Bruyere-Dobson circulation. Consequently, ozone does not transfer to the polar stratosphere. In reality, much depends on the type of La Niña [60]: during an eastern-type La Niña, strong SSWs occur, which may contribute to the strengthening of the Brewer-Dobson circulation and increase the concentration and total ozone content. The study of the influence of El Niño and La Niña of different types on stratospheric ozone will be the subject of further studies.

According to the modeling results, the influence of the trend on the SST increase is significant in the Northern Hemisphere, which is consistent with the "Arctic amplification" hypothesis, while the air temperature increase is also observed in the Arctic stratosphere [46,47]. An increase in ozone content is also observed, whereas it decreases in the tropics [46,47]. This process also contributes to the strengthening of the SSW, leading to the weakening of the SPV, and the Brewer-Dobson circulation, leading to an increase in the concentration and total ozone content. In reality, the atmosphere is affected not only by the increase in SST, but also by the level of CO₂, which, being a greenhouse gas, leads to an increase in tropospheric air temperature, especially in the Arctic [12,57]. There is also a decrease in air temperature in the stratosphere. Therefore, the influence of the trend for the increase of SST, as well as of global warming in general, on the polar stratosphere is ambiguous: it can lead both to the weakening of the SPL and increase of the total ozone content (especially in the Arctic), and vice versa - to the strengthening of the SPL and decrease of the total ozone content due to stratospheric cooling.

5. Conclusions

The results of numerical modeling and analysis of reanalysis data for the El Niño and La Niña phases allow us to draw the following conclusions.

(1) During El Niño, the SST increases by 3 degrees in the tropical Pacific Ocean, while during La Niña it decreases by 1.5-2 degrees. The air temperature in the troposphere during El Niño years over the Pacific Ocean and also near the poles increases by 2-3 degrees, which leads to deepening of the Aleutian depression and increase of the vertical heat flux to the stratosphere. During La Niña, the air temperature decreases and the heat flux stops. The peak of these phenomena occurs during the winter months.

(2) During the El Niño phase, the heat fluxes affect the zonal wind, resulting in a weakening of the SPV and its decay in February-March. This can be seen in the zonal wind at the boundary of the SPV, which at this time weakens and changes sign, indicating its reversal. During the La Niña phase, the SPV is stable according to the modeling results, but in reality the situation is less unambiguous - the stability of the SPV is determined by the type of La Niña and the processes not related to ENSO. The effect is stronger in the Northern Hemisphere than in the Southern Hemisphere.

(3) During the El Niño phase, the heat influx to the stratosphere leads to the increase of stratospheric air temperature and also increases the probability of SSW. These processes influence the zonal wind, which causes instability of the SPV, contributing to instability of the cold center over the poles and increasing ozone concentration. However, SSWs can be observed also during the La Niña phase, which can be related to the La Niña type and to the processes not related to ENSO. At the same time, the stratospheric response to El Niño occurs 2-3 months after reaching the El Niño maximum. This effect is stronger in the Northern Hemisphere than in the Southern Hemisphere.

(4) ENSO can contribute to the increase of ozone concentration and total ozone content, as can be seen from the modeling results for El Niño and La Niña scenarios and MERRA2 reanalysis data. During the La Niña phase, ozone concentration and total ozone content are determined by the type of La Niña and by processes not related to ENSO, such as the chemical processes that led to ozone depletion in March 2011 [16]. The modeling results show a decrease of ozone concentration and content in the tropical stratosphere by 2% and an increase in the polar stratosphere by 3%, indicating an increase in transport from the tropics to the poles due to weakening of zonal fluxes and strengthening of the Brewer-Dobson circulation due to atmospheric heating due to ENSO.

The results of numerical modeling and analysis of reanalysis data for the scenarios from the early 1980s and late 2010s allow us to draw the following conclusions.

(1) The SST for the period from 1980 to 2020 increased by 0.5 degrees on average over the planet, and by 1 degree in the Arctic. The air temperature in the troposphere is changing similarly. This supports the "Arctic amplification" hypothesis and global warming.

(2) Increasing SST leads to weakening of the zonal flow during winter months in the Northern Hemisphere according to reanalysis data, but modeling results do not give any significant weakening of the zonal wind. It is possible that these differences are due to the influence of not only SST but also CO₂ levels [12,57]. In the Southern Hemisphere, the zonal SPV flux is stable, and no significant response to the SST trend is observed.

(3) Model results give an increase in air temperature throughout the atmosphere except for the Southern Hemisphere stratosphere, and the Arctic stratosphere in spring, where a decrease is observed. The reanalysis data give warming of the troposphere and cooling of the stratosphere, but also warming in the Arctic stratosphere during the winter months, indicating the influence of "Arctic amplification".

(4) For ozone, the model results give an increase in concentration and total ozone in the tropical stratosphere, as well as in the Arctic stratosphere during the winter months, and in the Antarctic stratosphere during the summer months. The reanalysis data give a decrease of ozone concentration in the Antarctic stratosphere and also in the Arctic stratosphere in the spring months, which can be related to the chemical processes of ozone destruction.

The calculations of the residual circulation and wave activity allowed us to perform a physical analysis of the influence of ENSO and the SST trend on the atmospheric processes and make more detailed conclusions.

(1) The El Niño phase generates a strong ordered heat flux to the stratosphere, which can lead to a weakening of the temperature contrast between polar and tropical latitudes, as evidenced by the

vertical component of the residual circulation. This process affects the zonal wind, as can be seen from the decrease of the zonal wind speed in the polar regions. As a result, the zonal transport weakens and the meridional transport increases, as evidenced by the meridional component of the residual circulation, which increased from the equator to the poles, leading to further weakening of the zonal transport and SPV. Therefore, a stable SPV is most probable during the La Niña phase and the most unstable - during the El Niño phase. In addition, enhanced meridional transport leads to enhanced transport of heat and ozone from the tropical to the polar stratosphere via the Brewer-Dobson circulation, resulting in increased air temperature and ozone concentration in the polar stratosphere. During the La Niña phase, the heat flux to the stratosphere stops, resulting in an increase in the temperature contrast between the tropical and polar stratosphere, leading to a persistent SPV. As a result, zonal westerly transport increases and stratospheric ozone concentration over the poles decreases due to the absence of meridional fluxes. In the Arctic, the influence of ENSO is stronger than in the Antarctic because the zonal flow in the Antarctic is much stronger and the SPV is more stable than in the Arctic. The influence of the SST trend on the residual circulation, and hence on the Brewer-Dobson circulation, is much smaller, and appears mainly in the Northern Hemisphere.

(2) The heat flux associated with the El Niño phase may also contribute to the intensification of HSPs, which lead to an explosive effect in the stratosphere. SSW also attenuates temperature contrast, which affects zonal wind and weakens zonal transport. This contributes to the weakening, destabilization, and decay of the SPV. Observations show that in years with an unstable SPV, strong SSWs occurred, which may be related to heat fluxes into the stratosphere due to the Southern Oscillation. These processes also contribute to the increase of ozone concentration in the stratosphere of the Arctic and Antarctic.

(3) The decrease in the temperature contrast between polar and tropical latitudes in the stratosphere due to ENSO contributes to the enhanced wave activity flux, as seen in the calculations for the El Niño and La Niña scenarios - an increase in the meridional and vertical components at 20 km altitudes in the polar stratosphere, which indicate enhanced heat and mass flux through the planetary wave. This leads to a weakening of zonal transport and an increase in meridional transport that destroys the SPV. Wave activity flux divergence analysis shows increased convergence over the Northern Hemisphere during the winter months, and in the Southern Hemisphere during the summer months. Analysis of the amplitudes of waves with wave numbers 1 and 2 shows an increase in the amplitude of wave number 1 and a decrease in the amplitude of wave number 2, which is consistent with previous studies [41]. There is an increase in the wave heat flux and momentum of planetary Rossby waves from the equator to the pole, resulting in a weakening of the zonal flow and SPV, and an increase in the Brewer-Dobson circulation, which contributes to an increase in air temperature and total ozone content in the polar stratosphere. During the La Niña phase, due to the weakening of the heat flux to the stratosphere and an increase in the temperature contrast between the tropical and polar stratosphere, the heat and momentum flux through the planetary wave is weakened and the zonal flux is enhanced. This contributes to the weakening of the wave activity flux, stable SPV, and decreasing air temperature and ozone in the polar stratosphere. As for the SST trend, its influence on the wave activity flux and wave amplitudes is insignificant - there is just a weakening of the wave activity flux.

Thus, ENSO and the SST trend have a global impact on the atmosphere, affecting the stability of the SPV through the increase of heat fluxes to the stratosphere and SSW, as well as on the wave activity fluxes and stability of the planetary Rossby waves, the general atmospheric circulation and the total ozone content. But, in addition to ENSO and the SST trend, there are other processes affecting the SPV and Rossby waves, such as the Quasi-Decadal Oscillation and the North Atlantic Oscillation [63].

Author Contributions: Conceptualization, S.P.S. and V.Y.G.; methodology, S.P.S. and V.Y.G.; Formal analysis, A.R.J.; data curation, A.R.J.; writing—original draft preparation, A.R.J.; writing—review and editing, S.P.S.; visualization, A.R.J. All authors have read and agreed to the published version of the manuscript.

Funding: Russian Science Foundation project under the contract No №23-77-30008.

Data Availability Statement: The simulation and measurements data are available upon request to smyshl@rshu.ru.

Acknowledgments: We would like to thank European Centre for Medium-Range Weather Forecasts (ECMWF) for providing the ERA5 Data Set, and Met Office Hadley Centre for providing sea surface temperature and sea ice coverage data. CCM numerical experiments were carried out under State Task of the Ministry of Science and High Education of Russia for the Russian State Hydrometeorological University (project FSZU-2023-0004).

Conflicts of Interest: The authors declare no conflict of interest.

References

1. Taylor K.E., Williamson D., Zwiers F. The sea surface temperature and sea-ice concentration boundary conditions for AMIP II simulations // Program for climate model diagnosis and intercomparison, University of California, Lawrence Livermore National Laboratory, September 2000.
2. Hansen, J.; Sato, M.; Ruedy, R.; Lacis, A.; Oinas, V. Global warming in the twenty-first century: An alternative scenario. *Proc. Natl. Acad. Sci. USA* **2000**, *97*, 9875–9880.
3. Trenberth, K.; Hurrell, J.W. Decadal atmosphere-ocean variations in the Pacific. *Clim. Dyn.* **1994**, *9*, 303–319.
4. Collins, M.; An, S.-I.; Cai, W.; Ganachaud, A.; Guilyardi, E.; Jin, F.-F.; Jochum, M.; Lengaigne, M.; Power, S.; Timmermann, A.; The impact of global warming on the tropical Pacific Ocean and El Niño. *Nat. Geosci.* **2010**, *3*, 391–397, doi:10.1038/ngeo868.
5. Achuta Rao, K.; Sperber, K.R. Simulation of the El Niño Southern Oscillation: Results from the coupled model intercomparison project. *Clim. Dyn.* **2002**, *19*, 191–209.
6. Manatsa D., Mukwada G. A connection from stratospheric ozone to El Niño-Southern Oscillation // Scientific Reports (www.nature.com/scientificreports) (17 July 2017) | 7: 5558 | DOI:10.1038/s41598-017-05111-8
7. Guilyardi E., Wittenberg A., Fedorov A., Collins M., Wang C., Capotondi A., Oldenborgh G. J. van Stockdale T. Understanding El Niño in ocean-atmosphere general circulation models. Progress and Challenges. *Am. Meteorological Soc.* **2009**, *90*, 325–340.
8. Newman, P., A.; Nash, E., R.; Rosenfield, J.E. What controls the temperature of the Arctic stratosphere during the spring? *J. Geophys. Res.* **2001**, *106*, 19999–20010.
9. Jadin, E.A. Interannual variations of ozone above Europe and anomalies of ocean temperatures in Atlantic (In Russian). *Meteorol. Hydrol.* **1992**, *7*, 22–26.
10. Jadin, E.A. Long-periodic cyclicity of temperature of ocean surface, temperature of low stratosphere and ozone in moderate latitudes (In Russian). *Meteorol. Hydrol.* **1993**, *5*, 52–59.
11. Jadin, E.A. Arctic oscillation and interannual variations of temperature of Atlantic and Pacific oceans (In Russian). *Meteorol. Hydrol.* **2001**, *8*, 28–40.
12. Jakovlev, A.R.; Smyshlyaev, S.P.; Galin, V.Y. Interannual Variability and Trends in Sea Surface Temperature, Lower and Middle Atmosphere Temperature at Different Latitudes for 1980–2019. *Atmosphere* **2021**, *12*, 454. <https://doi.org/10.3390/atmos12040454>
13. Bell, C.; Gray, L.; Charlton-Perez, A.; Joshi, M.; Scaife, A. Stratospheric Communication of El Niño Teleconnections to European Winter. *J. Clim.* **2009**, *22*, 4083–4096.
14. Manatsa, D.; Mukwada, G. A connection from stratospheric ozone to El Niño-Southern Oscillation. *Sci. Rep.* **2017**, *7*, 5558.
15. Hu, D.; Tian, W.; Xie, F.; Shu, J.; Dhomse, S. Effects of meridional sea surface temperature changes on stratospheric temperature and circulation. *Adv. Atmos. Sci.* **2014**, *31*, 888–900.
16. Smyshlyaev, S.P.; Pogoreltsev, A.I.; Galin, V.J. Influence of wave activity on gaseous composition of stratosphere of polar regions. *Geomagn. Aeron.* **2016**, *56*, 102–116.
17. Dingzhu Hu, Wenshou Tian, Fei Xie, Jianchuan Shu and other. Effects of meridional sea surface temperature changes on stratospheric temperature and circulation // Advances in atmospheric science, vol. 31, July 2014, 888–900.
18. Horel JD, Wallace JM (1981) Planetary scale atmospheric phenomena associated with the Southern Oscillation. *Mon Weather Rev* 109:813–829
19. Halpert MS, Ropelewski CF (1992) Surface temperature patterns associated with the Southern Oscillation. *J Climate* 5:577–593. [https://doi.org/10.1175/1520-0442\(1992\)005<3C057:7:STPAWT>2.0.CO;2](https://doi.org/10.1175/1520-0442(1992)005<3C057:7:STPAWT>2.0.CO;2)
20. Hamilton K (1993) An examination of observed Southern Oscillation effects in the northern hemisphere stratosphere. *J Atmos Sci* 50:3468–3473
21. Domeisen DI, Garfinkel C, Butler AH (2019) The teleconnection of El Niño southern oscillation to the stratosphere. *Rev Geophys* 57:5–47. <https://doi.org/10.1029/2018RG000596>
22. Garcia-Herrera R, Calvo N, Garcia RR, Giorgetta MA (2006) Propagation of ENSO temperature signals into the middle atmosphere: a comparison of two general circulation models and ERA-40 reanalysis data. *J Geophys Res.* <https://doi.org/10.1029/2005JD006061>

23. Sassi F, Kinnison D, Bolville BA, Garcia RR, Roble R (2004) Effect of El-Nino Southern Oscillation on the dynamical, thermal, and chemical structure of the middle atmosphere. *J Geophys Res.* <https://doi.org/10.1029/2003JD004434>
24. Plumb, R. A. Stratospheric transport. *J. Meteor. Soc. Japan* 80, 793–809, doi:10.2151/jmsj.80.793 (2002).
25. Garny, H., Dameris M., Randel W., Bodeker G. & Deckert R. Dynamically forced increase of tropical upwelling in the lower stratosphere. *Journal of the Atmospheric Sciences* 68 (2011)
26. Forster, P. M. de F. & Shine, K. P. Radiative forcing and temperature trends from stratospheric ozone changes. *J. Geophys. Res.* 102, 10841–10855 (1997).
27. Barnston AG, Livezey RE (1987) Classification, seasonality and persistence of low-frequency atmospheric circulation patterns. *Mon Weather Rev* 115:1083–1126
28. Garfinkel CI, Hartmann DL (2008) Different ENSO teleconnections and their effects on the stratospheric polar vortex. *J Geophys Res Atmos.* <https://doi.org/10.1029/2008JD009920>
29. Smith KL, Kushner PJ (2012) Linear interference and the initiation of extratropical stratosphere–troposphere interactions. *J Geophys Res Atmos* 117: D13107. <https://doi.org/10.1029/2012JD017587>
30. Polvani LM, Waugh DW (2004) Upward wave activity flux as a precursor to extreme stratospheric events and subsequent anomalous surface weather regimes. *J Clim* 17:3548–3554
31. Sjöberg JP, Birner T (2012) Transient tropospheric forcing of sudden stratospheric warmings. *J Atmos Sci.* <https://doi.org/10.1175/JAS-D-11-0195.1>
32. Iza M, Calvo N, Manzini E (2016) The stratospheric pathway of La Nina. *J Climate* 29(24):8899–8914
33. Polvani LM, Sun L, Butler AH, Richter JH, Deser C (2017) Distinguishing stratospheric sudden warmings from ENSO as key drivers of wintertime climate variability over the North Atlantic and Eurasia. *J Climate* 30(6):1959–1969
34. Garfinkel CI, Butler AH, Waugh DW, Hurwitz MM (2012) Why might SSWs occur with similar frequency in El Nino and La Nina winters? *J Geophys Res* 117:D19, 106. <https://doi.org/10.1029/2012JD017777>
35. García-Herrera R, Calvo N, Garcia RR, Giorgetta M a. (2006) Propagation of ENSO temperature signals into the middle atmosphere: A comparison of two general circulation models and ERA-40 reanalysis data. *J Geophys Res* 111: D06101. doi: 10.1029/2005JD006061
36. Garfinkel CI, Hartmann DL (2007) Effects of the El Niño–Southern Oscillation and the Quasi-Biennial Oscillation on polar temperatures in the stratosphere. *J Geophys Res* 112: D19112. doi: 10.1029/2007JD008481
37. Butler AH, Polvani LM (2011) El Niño, La Niña, and stratospheric sudden warmings: A reevaluation in light of the observational record. *Geophys Res Lett.* doi: 10.1029/2011GL048084
38. Ineson S, Scaife AA (2009) The role of the stratosphere in the European climate response to El Niño. *Nat Geosci* 2:32–36. doi: 10.1038/ngeo381
39. Butler A.H., Polvani LM, Deser C (2014) Separating the stratospheric and tropospheric pathways of El Niño–Southern Oscillation teleconnections. *Environ Res Lett* 9:024014.
40. Butler A.H. El Niño and the stratospheric polar vortex // NOAA Climate.gov (science & information for a climate – smart nation) [Electronic resource]. – Mode of access: El Niño and the stratospheric polar vortex (climate.gov)
41. Sassi, F.; Kinnison, D.; Boville, B.A.; Garcia, R.R.; Roble, R. Effect of El Niño–Southern Oscillation on the dynamical, thermal, and chemical structure of the middle atmosphere. *J. Geophys. Res. Atmos.* **2004**, 109, D17108.
42. Hu, J.; Shen, Y.; Deng, J.; Jia, Y.; Wang, Z.; Li, A. Revisiting the Influence of ENSO on the Arctic Stratosphere in CMIP5 and CMIP6 Models. *Atmosphere* **2023**, 14, 785. <https://doi.org/10.3390/atmos14050785>
43. Vargin P.N., Kolennikova M.A., Kostykin S.V., Volodin E.M. Impact of sea surface temperature anomalies in the equatorial and North Pacific on the arctic stratosphere according to the INM CM5 climate model simulations // *Russian Meteorology and Hydrology*. 2021. T. 46. № 1.
44. Scott R., Polvani L. Internal variability of the winter stratosphere // *J. Atmos. Sci.* 2006. V. 63. P. 2758–2778.
45. Solomon S, Dahe Q, Manning M, et al. (eds) Intergovernmental Panel on Climate Change (IPCC), *Climate Change 2007*, Cambridge Univ Press: New York, 2007; pp. 996.
46. Prentice, I.C., Farquhar G.D., Fasham M.J.R., and other. The carbon cycle and atmospheric carbon dioxide, in *Third Assessment Report of the Intergovernmental Panel on Climate Change. Climate Change 2001: The Scientific Basis.*, edited by IPCC, pp. 183–238, Cambridge University Press, Cambridge, UK, 2001.
47. Stevenson, S. and B. Fox-Kemper 2012: Understanding the ENSO–CO₂ Link Using Stabilized Climate Simulations. *J. Climate*, 25, 7917–7936.
48. Zubov V.A., Rozanova I.V., Kiselev A.A., Karol' I.L., Rozanov E.V., Egorova T.A., Schmutz V. Simulation of Changes in Global Ozone and Atmospheric Dynamics in the 21st Century with the Chemistry–Climate Model SOCOL. *Izv. Atmos. Ocean. Phys.* **2011**. T. 47. № 3. C. 301–312.
49. Volodin E.M., Gritsun A.S. Simulation of Possible Future Climate Changes in 21 Century with Climate Model INM-CM5. *Izv. Atmos. Ocean. Phys.* **2020**. T. 56. № 3. C. 218–228.

50. Plumb R.A. On the Three-Dimensional Propagation of Stationary Waves // J. the Atmos. Sci., 1 February 1985, VOL. 42, NO. 3, pp. 217-229.
51. Kinoshita T., Tomikawa Y., Sato K. On the Three-Dimensional Residual Mean Circulation and Wave Activity Flux of the Primitive Equations // Journal of the Meteorological Society of Japan, Vol. 88, No. 3, pp. 373-394, 2010.
52. Galin, V.Y.; Smyshlyaev, S.P.; Volodin, E.M. Combined Chemistry–Climate Model of the Atmosphere. *Izv. Atmos. Ocean. Phys.* **2007**, *43*, 399–412.
53. Smyshlyaev, S.P.; Galin, V.Y.; Shaariibuu, G.; Motsakov, M.A. Modeling the Variability of Gas and Aerosol Components in the Stratosphere of Polar Regions, *Izv. Atmos. Ocean. Phys.*, **2010**, *46*, 265–280.
54. Smyshlyaev, S.P.; Galin, V.Y.; Blakitnaya, P.A.; Jakovlev, A.R. Numerical Modeling of the Natural and Manmade Factors Influencing Past and Current Changes in Polar, Mid-Latitude and Tropical Ozone. *Atmosphere* **2020**, *11*, 76, doi:10.3390/atmos11010076.
55. Smyshlyaev S.P., Geller M.A., Yudin V.A. Sensitivity of model assessments of high-speed civil transport effects on stratospheric ozone resulting from uncertainties in the NO_x production from lightning // Journal of Geophysical Research. 1999. T. 104. № D21. C. 26401-26417.
56. Sukhodolov T., Rozanov E., Ball W.T., Schmutz W., Peter T., Bais A., Tourpali K., Shapiro A.I., Telford P., Smyshlyaev S., Fomin B., Sander R., Bossay S., Bekki S., Marchand M., Chipperfield M.P., Dhomse S., Haigh J.D. Evaluation of simulated photolysis rates and their response to solar irradiance variability // Journal of Geophysical Research. 2016. T. 121. № 10. C. 6066-6084.
57. Dianskii, N.A., Galin, V.Ya., Gusev, A.V., Volodin, E.M., Iakovlev, N.G., Smyshlyaev, S.P. The model of the Earth system developed at the INM RAS, Russian Journal of Numerical Analysis and Mathematical Modelling. 2010, 25, 419-429.
58. Weather and Climate Change [Electronic Resource] / Met Office. Available on line: http://https://www.metoffice.gov.uk/hadobs/hadgem_sst/data/download.html (accessed on March 20, 2022).
59. Jakovlev, A.R.; Smyshlyaev, S.P. Numerical Simulation of World Ocean Effects on Temperature and Ozone in the Lower and Middle Atmosphere. *Russ. Meteorol. Hydrol.* **2019**, *44*, 594–602.
60. Jakovlev, A.R.; Smyshlyaev, S.P. Impact of the Southern Oscillation on Arctic Stratospheric Dynamics and Ozone Layer. *Izv. Atmos. Ocean. Phys.* **2019**, *55*, 86–99.
61. Gelaro, R.; McCarty, W.; Suarez, M.J.; Todling, R.; Molod, A.; Takacs, L.; Randles, C.; Darmenov, A.; Bosilovich, M.; Reichle, R.; et al. The Modern-Era Retrospective Analysis for Research and Applications, Version 2 (MERRA-2). *J. Clim.* 2017, 30, 5419–5454.
62. Kolennikova, M.; Gushchina, D. Revisiting the Contrasting Response of Polar Stratosphere to the Eastern and Central Pacific El Niños. *Atmosphere* 2022, 13, 682. <https://doi.org/10.3390/atmos13050682>.
63. Gushchina, D.; Kolennikova, M.; Dewitte, B.; Yeh, S.-W. On the relationship between ENSO diversity and the ENSO atmospheric teleconnection to high-latitudes. *Int. J. Climatol.* 2021, 42, 1303–1325.
64. Ayarzagüena, B.; Ineson, S.; Dunstone, N.; Baldwin, M.; Scaife, A. Intraseasonal Effects of El Niño–Southern Oscillation on North Atlantic Climate. *J. Clim.* 2018, 31, 8861–8873.
65. Pogoreltsev A.I., Savenkova E.N., Aniskina O.G., Ermakova T.S., Chen W., Wei K. Interannual and intraseasonal variability of stratospheric dynamics and stratosphere-troposphere coupling during northern winter // Journal of Atmospheric and Solar-Terrestrial Physics, 136 (2015), pp. 187–200.

Disclaimer/Publisher’s Note: The statements, opinions and data contained in all publications are solely those of the individual author(s) and contributor(s) and not of MDPI and/or the editor(s). MDPI and/or the editor(s) disclaim responsibility for any injury to people or property resulting from any ideas, methods, instructions or products referred to in the content.